KUMUD KOIRALA

Adaptive Self-Interference Cancellation in Full-Duplex Radio

Master of Science thesis

ABSTRACT

Full-duplex transmission is a scheme where the transmitter and the receiver of a transceiver can transmit and receive simultaneously using same carrier frequency. Full-duplex transmission theoretically doubles the spectral efficiency and avoids using the separate frequency bands for transmitted and received signal. Full duplex transmission suffers from the self-interference because of the powerful transmit signal coupling back to its own receiver chain. This self-interference signal should be mitigated for the efficient operation of the full duplex radio.

This thesis work includes the experiment on the cancellation of self-interference signal induced during the full duplex transmission. LMS algorithm has been adopted for the channel estimation of self-interference channel and the self-interference cancellation has been carried out at the baseband level. Rician channel has been used as a self-interference channel with a high power in the line of sight direction.

Effect of K parameter of Rician channel and LMS algorithm on self-interference cancellation has been studied in this thesis work. The simulation work has been carried in a LabVIEW™ environment. Different level of attenuation has been observed by varying the number of samples for estimation/cancellation, step size and the length of estimation filter. In this thesis, the used figure of merit is the output power of self-interference digital canceller (error signal).

PREFACE

This thesis has been written for the completion of Master of Science (Technology) in Electrical Engineering from Tampere University of Technology.
I would like to thank my examiner Professor Mikko Valkama for his support and providing me with a thesis topic. I would also like to thank Electronics and communication Engineering department for providing LabVIEW™ tool to carry out this thesis work. I would like to thank my supervisor Sudharsan Srinivasan for guiding me throughout this thesis work. I will also like to thank Dani Korpi for his help during this thesis work.
I would like to express my deep gratitude towards my family and friends.

Tampere, 25.05.2016

Kumud Koirala

CONTENTS

LIST of ABBREVIATIONS

AP	Access Point
ADC	Analog to Digital Converter
CSMA/CA	Carries Sense Multiple Access with Collision Avoidance
DAC	Digital to Analog Converter
EMW	Electro Magnetic Wave
FD	Full Duplex
FDD	Frequency Division Duplexing
HD	Half Duplex
LMS	Least Mean Square
PU	Primary Users
PN	Pseudo Noise
QAM	Quadrature Amplitude Modulation
QPSK	Quadrature Phase Shift Keying
RACH	Random Access Channel
RLS	Recursive Least Square
RTS/CTS	Request to Send/Clear to Send
SI	Self Interference
SIR	Signal to Interference Ratio
SISO	Single Input Single Output
SOI	Signal of Interest
SU	Secondary Users
TDD	Time Division Duplexing

LIST of FIGURES

1 Introduction

Wireless technology has been exponentially growing from the past years. With introduction of wireless telegraph in 1896 [1], demand for more advance wireless technology has been increasing day by day. As more portable devices are carried by people, there is more demand for data services which includes audio and video services.

Most of the wireless network operates in the half duplex mode. One of the duplexing method used in wireless communication is known as frequency division duplexing (FDD). In this method communication occurs in two separate frequency bands. Each transmitter/receiver uses separate frequency bands to communicate with distant transmitter/receiver at the same time. Time division duplexing (TDD) uses same frequency band for transmitter/receiver in different time slot separated by guard interval, in order to communicate with the distant transmitter and receiver.

Currently most of the available frequencies are already in use. Even unlicensed bands like the ISM bands are in use by different wireless devices because of which there is a high congestion in the frequency spectrum. This situation has strongly motivated engineers and scientist to develop more spectrally efficient system.

Full-duplex (FD) means to receive and transmit data at same carrier frequency and at same time unlike the half duplexing method like TDD or FDD. FD radio fulfills the requirement of high throughput and spectral efficiency. Self -interference is major problem that has to be faced when implementing such kind of FD radio system [2]. Self- Interference (SI) occurs when receiver receives signal of interest from a distant transmitter along with signal from its own transmitter chain, thus interfering with the signal of interest SOI [2].

FD radios may use same antenna or a different antenna to transmit /receive data. Use of separate transmitting and receiving antenna provides high level of isolation than using a single antenna [3]. In [2], author has purposed three antennas, two for transmitting and one for receiving in order to cancel out the SI signal in space, by placing receiving antenna asymmetrically in between two transmitting antennas. In [3], author has used a single antenna where the transmitted power couples to receiver chain through a circulator leakage, reflections due to impedance mismatch and multipath components. Even though power of multipath component is quite low, leakage and reflected power creates more interference to receiving chain. The author [3] has purposed a balanced feed network to mitigate those interfering power.

The power of the transmitting antenna couples back to antenna of receiving chain and superimposed with the signal of interest. Adaptive cancellation algorithms like Least

Mean Square (LMS) can help in cancelling out the interfering signal from the SOI using digital cancellation technique. The baseband SI cancellation is better when high power of transmitted signal couples back to the receiving antenna. This is because high power level of SI signal gives good channel estimates and thereby reducing the channel estimation error. According to [4], Rician channel with powerful LOS component and low power multipath component models SI channel accurately. The K parameter in the Rician channel controls the power of LOS component compared to the power of multipath components. The higher the value of K, more power is coupled to the receiving chain from the transmitter through line of sight. This models closer proximity of transmitting and receiving antenna.

In this thesis, we studied SI cancellation using LMS algorithm. The experiment for SI cancellation was conducted using LabVIEW™ tool. LabVIEW™ is a powerful graphical programming tool developed by the National Instrument. It has been designed specifically for engineers and scientist to increase productivity. Graphical programming syntax used in LabVIEW environment is easier to visualize, create and design [5]. LabVIEW provides various tools for wireless communication providing more complex library function that can be used in simulating RF transceiver.

Full Duplex radio gives capability of theoretically doubling spectral efficiency compared to half duplex system as FD employs same channel to transmit and receive data at same time [6]. Full Duplex can be used to solve the hidden node problem [7]. Access Point operating in a full duplex mode can listen to a channel for any incoming data and can transmit at same time, thus avoiding collision. This increases throughput and fairness of the channel.

Similarly, full-duplex can be used in cognitive radio for spectrum sensing [8]. Secondary users can constantly sense the spectrum for primary users and can avoid interruption for any incoming data for primary users. Thus full duplex radio can help prevent any collision between the primary users and secondary user's data.

In chapter 1, we will discuss about the FD system, challenges while implementing it, and the application of FD radio system. Similarly, in chapter 2, we will discuss about different self -interference cancellation techniques. This chapter covers active and passive cancellation technique used for cancelling out the SI signal. In chapter 3, Rician SI channel model used in the simulations has been discussed. In chapter 4, adaptive self -interference cancellation technique has been discussed which is based on the LMS algorithm. This chapter covers detail about real value processing of LMS algorithm. In chapter 5, a transceiver model has been proposed that was design in LabVIEW. In chapter 6, waveform simulation results have been analyzed. In chapter 7 we will end the thesis with conclusion and future work.

1.1 Full Duplex System

One of the most widely used equations in communication field was derived by Shannon which gives the theoretical maximum capacity of a communication link when SNR and bandwidth are known. The Shannon capacity formula for a half-duplex link as given in [9] can be expressed as

$$C_{HD} = B \log_2 (1 + SNR) \tag{1.1}$$

Where C is capacity in bits/sec, B is bandwidth in Hertz (Hz) and SNR is signal to noise ratio. The capacity of half duplex system is governed by the equation (1.1). The received signal at the antenna is resultant of self-interfering signal and the SOI. The signal propagating from the distant transmitter gets highly attenuated when it reaches at the receiver end. Due to the closer proximity of transmitting and receiving antenna of a transceiver, SI signal has higher power than that of SOI at the receiving end. This causes the receiver end to interpret SOI as a noisy signal in the presence of SI signal. Full duplex system can operate efficiently when the self-interference signal is cancelled out.

Figure 1.1: A point to point communication link.

In *Figure 1.1*, two transceivers are communicating with each other. Assuming both transceivers TRX_A and TRX_B operating in the HD mode and $SNR_{A,B}$ and $SNR_{B,A}$ is the signal to noise ratio at receiving side, then the channel capacity of each link in presence of additive white Gaussian noise is given by

$$C_{A,B} = B \log_2 (1 + SNR_{A,B}) \tag{1.2}$$

$$C_{B,A} = B \log_2 (1 + SNR_{B,A}) \tag{1.3}$$

Assuming equal data rate in both directions, capacity for HD link is given by

$$C_{HD} = B \log_2 (1 + min[SNR_{A,B}, SNR_{B,A}]) \tag{1.4}$$

For HD link, the capacity is limited by the minimum SNR at either side of the link. The self-interfering signal can be removed by using antenna cancellation technique at band pass level. There can be still some *residual SI signal with power P_{res}* after antenna cancellation, which can be removed using digital cancellation at baseband level. In the presence of SOI, noise and residual SI, signal to noise ratio can be defined as

$$SNR_{A,B} = SNR_{B,A} = \frac{P_{SOI}}{P_N + P_{res}} \tag{1.5}$$

Where, P_{SOI} and P_N is power of SOI and noise respectively.

For ideal FD link, we can assume *complete cancellation of SI signal ($P_{res} = 0$)* while maintaining constant SNR, which results in theoretical capacity of a full duplex radio given by

$$C_{FD} = B \log_2\left(1 + SNR_{B,A}\right) + B \log_2\left(1 + SNR_{A,B}\right) \tag{1.6}$$

Assuming equal SNR in both directions, i.e. $SNR_{A,B} = SNR_{A,B} = SNR_{FD}$, equation (1.6) becomes

$$C_{FD} = 2B \log_2\left(1 + SNR_{FD}\right) \tag{1.7}$$

Equation (1.7) gives the theoretical upper bound capacity for a FD system. It can be seen that spectral efficiency has been doubled compared to that of HD link with same available bandwidth. It is important to achieve same SNR in FD radio as in HD radio for the capacity to be doubled. It is to be noted that FD system can work at full efficiency if and only if both the transceiver, A and B sends and receives the data at the same time.

1.2 Challenges in Implementation

As explained in previous sections, self-interference is major problem while implementing FD radio [2, 4] because of the superimposition of the transmitted signal with the signal of interest at the same frequency band.

The challenging part while implementing adaptive cancellation depends on the choice of adaptive filtering algorithm. The right parameter of algorithm has to be fixed to guarantee cancellation. For example, LMS algorithm performance varies with the different step size and length of the estimation filter [10] giving different result for SI cancellation.

Another challenging part while implementing SI cancellation is coupling channel between transmitter and receiver of a transceiver. Small scale fading channel like Rician channel has been used in this experiment. Parameter for the channel should be chosen with care, so that it perfectly imitates the coupling between the transmitter and receiver of a transceiver. For example, Rician channel parameter "K" is the ratio of the power of signal from line of sight to the power from other multipath components. So higher the ratio "K" means high power of self-interfering signal is directly coupling from transmitter to the receiver chain through line of sight. This also means that the distance between the transmitting antenna and receiving antenna is quite less [4].

Since channel condition between transmitting and receiving antenna doesn't change much with time because of fixed antenna, there is no Doppler spread. But if intermediate object or scatters position changes very fast, the Doppler spread is very high and the

coherence time is quite small [11]. This results in rapid change of channel impulse response and thus good channel estimation is required when there is a presence of high Doppler spread because of the moving scatters [11].

1.3 Nomenclature

All the vector quantity in this thesis is represented with the bold and italics letters and the scalar quantity is represented with normal letters. The notation $(.)^{\wedge}$ and $(.)^{*}$ represents the instantaneous value and complex conjugate of the given quantity respectively. The operator $(.)^{H}$ and $\otimes$ represents the Hermitian transpose and convolution respectively.

1.4 Application of Full Duplex Radio

FD radio has several applications. The applications of FD radio are listed here.

- Solving Hidden Node Problem
- Full duplex base station
- Cognitive radio
- Security

1.4.1 Solving Hidden Node Problem

Hidden node problem occurs when the two nodes which are out of range, cannot listen to the transmission of each other and thus collision occurs.
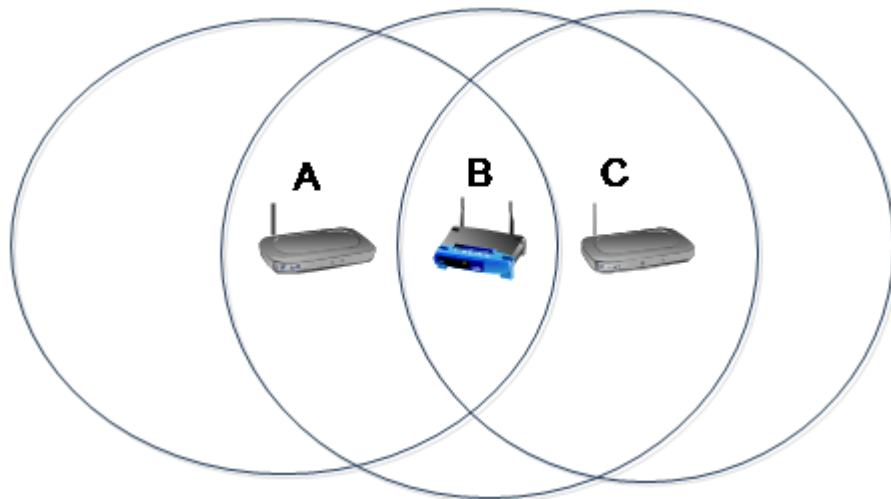

Figure 1.2: A picture showing the B as an AP, A and C as a two nodes communicating with each other.

In *Figure 1.2*, two nodes are trying to communicate with access point B. Node B can listen to transmission of A and C which are within range of B. A and C cannot listen to each other because they are outside of hearing zone. A is trying to send data to B, but C

is unaware of any transmission in progress, as it cannot sense medium. Thus if C tries to send a packet at this time, there can be collision.

If somehow B is full duplex node, it can receive data from node A, and at same time inform the node C about current data reception in progress, thus avoiding collision. Moreover, node A and C need not to be a full duplex node. Thus simultaneous transmission and reception avoids collision and this will increase the throughput of network.

In [7] author has mentioned the SI cancellation using signal inversion technique and adaptive cancellation. The paper presents MAC design control for full duplex node. It has been observed that a full duplex node increases fairness of network from 0.85 to 0.98 and also increases throughput of downlink and uplink by avoiding collision in the full duplex nodes.

In half duplex mode, where the multiple nodes have to communicate with the same AP, there arises congestion problem. Full duplex helps to mitigate these problems by transmitting and receiving from the same node with the AP [7].

1.4.2 Full Duplex Base Station

A base station operating in a full duplex mode can serve two mobile users at a same time without FDD or TDD. To utilize this technique, there should be proper spatial separation between two mobile. This is due to the fact that transmitting uplink mobile user can interfere to the receiving one in the downlink.

Full duplex base station cannot be used in full capacity where number of mobile users are less. As mentioned in [12], it is ineffective to use full duplex radio in a Femtocell where number of users are quite less.

Full duplex system is efficient when there is equal amount of traffic to receive and transmit. Due to this fact, full- duplex system should be implemented in such base station where transmission and reception happens simultaneously and load is divided evenly between the transmitting and receiving end.

Digital cancellation requires the proper channel estimation in order to cancel out the SI signal. In a RACH (Random access channel), it is highly unlikely to start a new transmission when there is ongoing receiving process. This is because some part of receiving signal has to be used for channel estimation for further SI cancellation [13].

1.4.3 Cognitive Radio

Secondary user uses available spectrum from primary user in a cognitive radio. During this stage, Secondary user has to check if it is blocking any transmission for the primary user. This is usually done using TDD by stopping transmission for certain interval and

listening for any incoming reception for primary user. This old traditional method is quite ineffective because of the collision that may occur if the data transmission occurs between these ceased intervals.

In [2] author has proposed full duplex system to counter such kind of problem. In a full duplex mode transmission and reception can happen simultaneously, so basically it is possible to listen to the incoming transmission for the primary user in particular channel while the secondary user uses the same channel for transmission. Receiver can be used for sensing spectrum for primary while there is ongoing transmission for the secondary user.

Since SI cancellation for cognitive radio is required for spectrum sensing, the requirement of SI cancellation level in this case, need not to be high as required in any other transceiver. Throughput in cognitive radio network increases when using this full duplex sensing scheme in comparison to TDD scheme [8].

1.4.4 Security

Full duplex Radio also provides security measures while communicating between two nodes. Self-Interfering signal can be used as a jamming signal in order to protect data and to ensure data is received by intended user.

Transmitting a jamming signal while receiving SOI, data can be securely transferred. As jamming signal structure is known to the particular recipient, it will be easy to cancel out the jamming signal while restoring the SOI. At same time, for other user jamming signal will be heard, rather than low power SOI.

In [14], similar type of application has been discussed to prevent eaves dropping by the unwanted recipient. Antenna cancellation in [14] has shown increment in network secrecy when unknown structure of jamming signal was used.

In [15], FD MIMO transceiver is assumed where receiver transmits the jamming signal to degrade the eavesdropping channel while receiving the data. It is shown that the FD transceiver can be used to improve the secrecy of channel along with high data rate.

2 Self-Interference Cancellation Technique

There are number of self-interference cancellation technique that can be found in various research papers. They are generally categorized in two types, namely *active and passive cancellation*. Some previous work in this field [4,6,7,13,16,17,18] mainly uses passive, active or cascade of both cancellation technique so as to reduce self-interference signal level.

As mentioned in [19], complete self-interference cancellation is not possible because of the impairments of the radio circuits. Impairments like transmitter and receiver non linearity, transmitter and receiver phase noise, ADC quantization noise can have severe impact on the SI cancellation level. Generally, power amplifier in transmitter chain introduces non linearity in a circuit and this can be detrimental with increase in transmission power [17]. Therefore, a single cancellation scheme might not be sufficient to reduce the SI signal below noise floor due to which cascade of different cancellation schemes is suggested in various research papers [17]. This section covers some of the SI cancellation technique that has been implemented so far.

2.1 Active Cancellation

Active SI cancellation technique is a process in which an inverse of interfering signal is generated and added to the self-interference signal in order to remove the interference. Active cancellation can be done in both baseband and band pass signal. It is generally classified as follows.

- Antenna Cancellation
- Analog Cancellation
- Digital Cancellation

2.1.1 Antenna Cancellation

This cancellation technique is based on the fact that the two signals adds up in the space resulting in either constructive or destructive signal [20]. Transmission signal (self- interfering signal) is divided and transmitted using two antennas TX1 and TX2 as shown in *Figure 2.1*. The receiving antenna RX is placed at null point of two transmitting antennas TX1 and TX2, in such a way that the signal transmitted from the two antennas results in destructive combination at receiving end, thus mitigating some of the self-interference signal. After reducing self-interfering signal, the RX will be able to hear weaker signal of interest.

Antenna cancellation technique, as proposed in [2] utilizes three antennas, two for transmitting and one for receiving in a single node. Two transmitting antenna are kept at a distance of d and $_{d + \lambda/2}$ from the receiving antenna as shown in *Figure 2.1* [2]. The self-interfering signal from the two transmitting antennas adds up destructively at the receiving point.
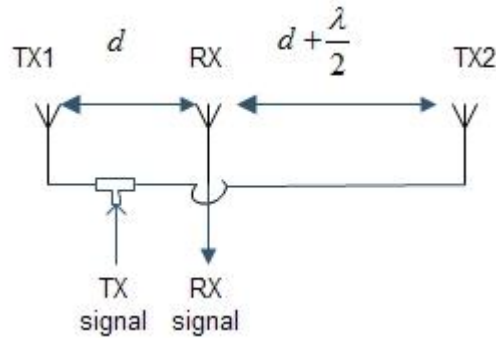
Figure 2.1:Antenna setup for Antenna cancellation.

Additionally, antenna cancellation can only be achieved, if signal level from the transmitting antenna (TX1) which is close to the receiving antenna is attenuated to match with the signal level from other transmitting antenna (TX2) which is far away from the receiving antenna [2].

As mentioned in [2], maximum cancellation that can be achieved for a 5 MHz with center frequency of 2.48GHz was 60.7dB when there is a perfect matching. In case of 1dB mismatch, the cancellation was observed to be 20dB.

Large SI signal voltage level covers most of dynamic range of the ADC which causes the low level SOI to suffer from large quantization noise [18]. Antenna cancellation reduces self-interference signal so that the ADC can accurately represent signal of interest. The amplitude or power of signal of interest is quite low with respect to interference signal and dynamic range of ADC is the limiting factor when representing the signal of interest. So it's important to cancel out the interference in RF, so that the ADC can represent the SOI with enough precision [16].

Antenna separation method is not quite useful for a wideband signal where phase shifting is not uniform over entire bandwidth reducing the SI attenuation level [4]. It has been mentioned in [4] that 40dB attenuation was achieved for RF signal having 2MHz bandwidth, whereas 10dB attenuation was observed for 20MHz bandwidth both centered at 2.4GHz carrier frequency.

2.1.2 Analog Cancellation

Analog cancellation technique implies cancellation of SI signal at RF level by adding up a phase inverted signal [6]. In [6], author has purpose analog cancellation technique in which an additional auxiliary transmitter chain has been used for self-interference signal cancellation. In *Figure 2.2*, original baseband signal $u(n)$ has been up converted and transmitted using TX1 antenna resulting in band pass signal $u(t)$. The self-interference channel h_{SI} couples power in the receiving antenna RX thus interfering with signal of interest.

The auxiliary transmitter chain TX2 uses a wired channel having response h_{wire} with a canceller signal $d(t)$. It can be observed from the *Figure 2.2*, that the received signal $y(t)$ is the result of addition of three different signal including AWGN signal n and can be defined by the equation (2.1)

$$y(t) = h_{SI} \otimes u(t) + h_{wire} \otimes d(t) + n \tag{2.1}$$
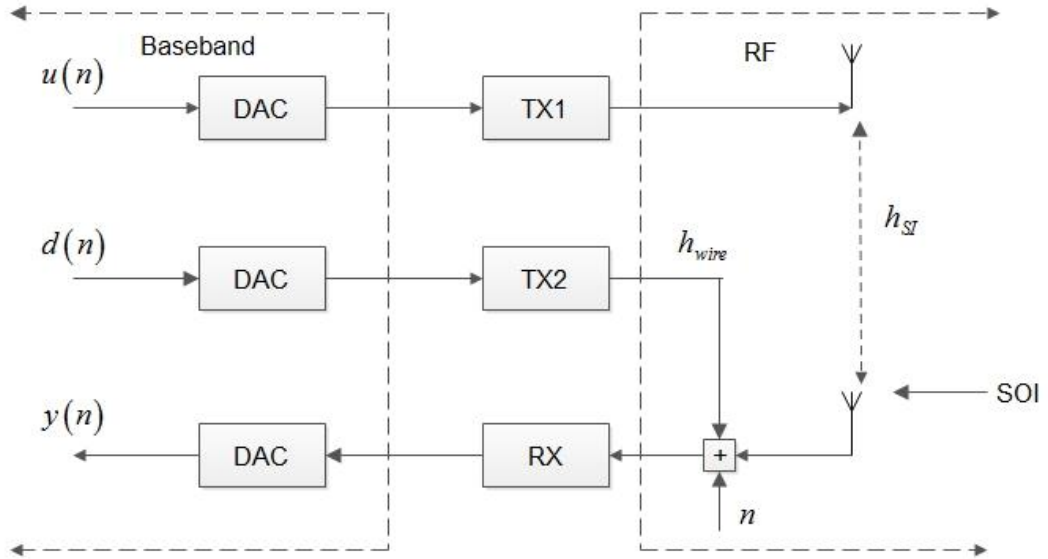
Figure 2.2: Analog Cancellation Scheme utilizing two transmitting antenna and one receiving antenna.

It can be seen from equation (2.1), in order to cancel out term $h_{SI} \otimes u$ and $h_{wire} \otimes d$, h_{wire} must be equal to $-\hat{h}_{SI} u / \hat{h}_{wire}$ where $\hat{h}_{SI}$ and $\hat{h}_{wire}$ are the noisy estimation of h_{SI} and h_{wire} because of the estimation error, respectively.

The experiment in [6] was conducted with antenna separation of 20cm and 40 cm with a fixed distance of 6.5 cm between two nodes. The SI cancellation was observed to be 33 dB when separation was 20 cm where as 31dB cancellation was observed when separa-

tion was 40 cm. This is because greater the separation between the transmitting and receiving antenna, greater will be the estimation error because of the lower power SI signal coupling back to the receiving antenna. This will decrease the SI cancellation level.

2.1.3 Digital Cancellation

Digital cancellation is technique in which self-interference is mitigated at the digital baseband level [2]. A prediction of received SI is formed, provided that transmitted samples are already known inside receiver where cancellation is performed. In [17] author has proposed a nonlinear digital cancellation technique along with RF cancellation which can be readily modified for the linear digital cancellation as shown in *Figure 2.3*.

In [17] *Figure 2.3*, x_n is original digital baseband transmit signal. The multipath channel between the transmitting antenna and receiving antenna is defined by the impulse response h_n . The estimated SI channel can be defined with an impulse response of $\hat{h}_n$. The estimated channel is modeled as FIR filter with L number of delays and the weight w_0 to w_{L-1} . The length of the estimation filter and tapping point can be different according to channel condition or multipath component. s_n is signal of interest which gets superimposed with self-interference signal and w_n is additive white Gaussian noise. So from *Figure 2.3*, total self-interference signal can be defined as

$$x_n^{SI} = x_n \otimes h_n + s_n + w_n \qquad (2.2)$$

Similarly the reference signal x_n is passed through the estimated channel to generate signal $\hat{x}_n^{SI}$ which is used for cancelling out the self-interference signal and can be defined as

$$\hat{s}_n = x_n^{SI} - \hat{x}_n^{SI} \qquad (2.3)$$

The self-interference estimate $\hat{x}_n^{SI}$ is defined as

$$\hat{x}_n^{SI} = x_n \otimes \hat{h}_n = \sum_{k=0}^{L-1} w_k x_{n-k} \qquad (2.4)$$

After RF cancellation there is still some residual SI, which can be mitigated using digital cancellation at baseband [16]. Any adaptive estimation algorithm for example, LMS or RLS algorithm can be implemented to estimate a channel from residual SI signal.

It has been observed in [18] that amount of SI cancellation is directly proportional to the power of SI signal which gives the better estimation of SI channel by lowering the channel estimation error.

Linear signal processing method for digital cancellation cannot mitigate the effect of non-linearity introduce by the transceiver chain. This is due to the fact, that the reference sample for the digital cancellation exist only in the digital state of the transmitter chain, and does not include any non-linearity introduced by the component of transmitter chain, for example, power amplifier. This decreases the SI cancellation level by the digital cancellation method.
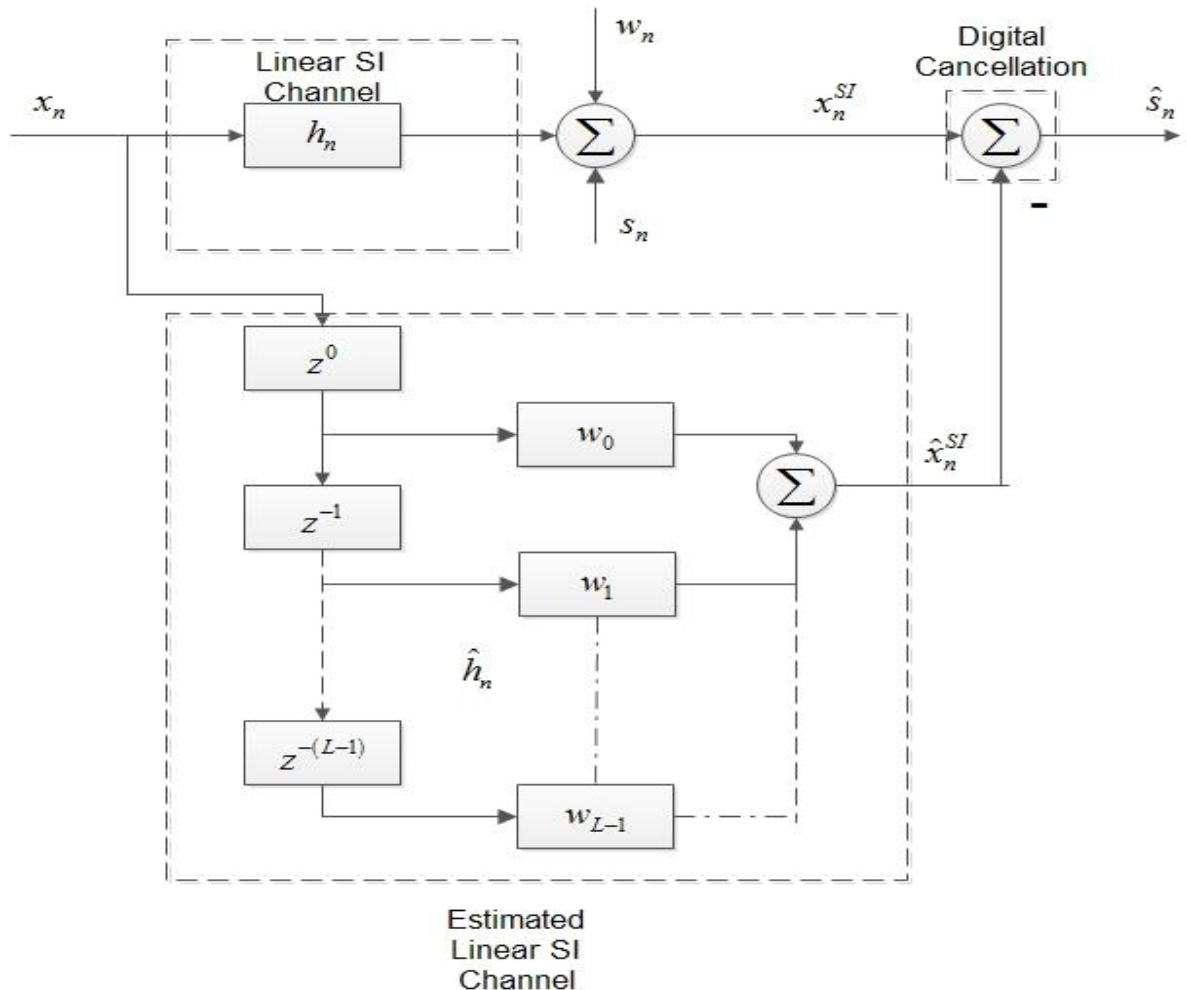
Figure 2.3: A digital cancellation technique where the SI signal is regenerated and subtracted from the overall received signal at digital baseband.

The level of SI attenuation also depends on the number of training samples used for digital cancellation. Similarly, the length of the channel estimation filter should be long enough to produce good estimation.

2.2   Passive Cancellation

Passive cancellation is a technique, in which energy of a transmitted signal from a node is directed to a receiver at a different node, by using a directional antenna in order to

suppress self-interference signal [16]. Similarly, path loss between the transmitting and receiving antenna also provides passive SI suppression.

In [16], author mentions about the directional diversity as one of the method of the passive cancellation. This cancellation technique uses antenna isolation between the separate antennas or circulator isolation between shared antennas [17]. In directional diversity, node operating at full duplex completely relies on directional antenna for transmitting and receiving. The performance of this link depends on angular separation between these two antennas.

The larger the angle between the two antennas, more isolation is achieved between transmitting and receiving ends. A regular 2.4GHz patch antenna for both transmitter and receiver was used in [16]. It has been observed that the passive cancellation shows better performance in FD radio over HD radio even in the absence of extra hardware for cancellation.

Similarly, in [16] when using omnidirectional antenna there is not much angular separation due to which there is very low SIR when compared with the case using omnidirectional antenna. So the choice of antenna type is also important, when there is requirement for passive cancellation.

In [6] author has used antenna separation technique, in which path loss between transmitting and receiving antenna provides certain level of SI suppression. Since the distance between these two antennas is not high enough and does not contribute enough path loss, author has used active cancellation technique as well.

3 Self-Interference Channel Modeling

Self-Interference Channel refers to medium between transmitting and receiving antenna. Channel characteristic depends on distance between transmitting and receiving antenna, multipath component and scatters present between these two antennas. The profile of the received signal can be obtained from the transmitted signal if a channel model is known between these antennas.

The simplest channel between the transmitting and receiving antenna can be consider when there is only presence of line of sight without any obstacle between them. The power of signal attenuates along with the distance due to which the received power is always less than transmitted power. Path loss model are deterministic in nature and depends on the antenna height and environment.

Some part of the transmitted signal gets lost during propagation because of the absorption, reflection, scattering and diffraction caused by any intermediate object present between the transmitting and receiving antenna. This phenomenon is termed as shadowing or large scale fading. Large scale fading is the change in the received signal power around the nominal value, based on different path loss model, due to the movement of the receiver, transmitter or both over large areas.

Shadowing is modeled as a zero mean white Gaussian distributed variable in a macro cell with a standard deviation of σ_s also known as location variability. The parameter σ_s introduces a shadowing margin l_s whose probability density function is defined as

$$p(l_s) = \frac{1}{\sigma_s \sqrt{2\Pi}} \; exp\left[-\frac{l_s^2}{2\sigma_s^2} \right]$$

(3.1)

Small scale fading model assumes that a transmitted signal reaches receiving antenna through multipath because of reflection caused by an intermediate object present between these antennas. The multiple versions of the transmitted signal arrive at the receiver at different times. These multipath waves combine at the receiver to give a resultant signal which varies widely in amplitude and phase. The resultant amplitude depends on the propagation time, intensity and the bandwidth of the transmitted signal [21].
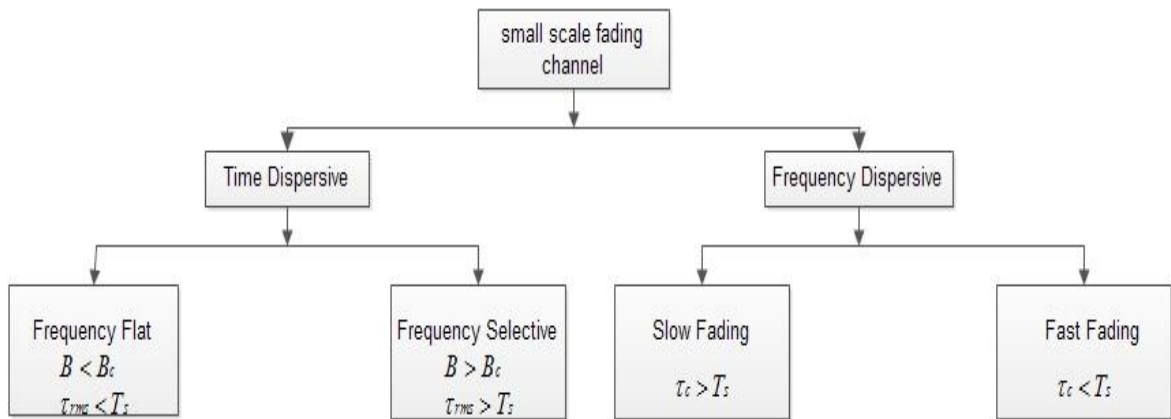
Figure 3.1:Classification of small scale fading channel.

As shown in *Figure 3.1*, the multipath channel bandwidth can be quantified as a coherence bandwidth (B_c) which depends on the multipath structure of the channel. Coherence bandwidth is the measure of the range of frequencies for which the signals are strongly correlated in amplitude. The received signal will be distorted if a signal bandwidth (B) is greater than bandwidth of the multipath channel, but the strength of the received signal will not fade much over a local area. If the transmitted signal has smaller bandwidth than that of channel, amplitude of signal will change rapidly but the signal will not be distorted.

Multipath delay spreads lead to time dispersion and frequency selective fading whereas Doppler spread leads to frequency dispersion and time selective fading. Delay spread is time measure after which received signal power can be neglected. Generally RMS values of delay spread (τ_{rms}) is consider while analyzing the channel characteristics. As shown in *Figure 3.1*, fast fading occurs when the coherence time (τ_c) is smaller than the symbol period (T_s) where as slow fading occurs when the coherence time is greater than the symbol period.

3.1 Tapped Delay Line

Small scale variation of radio signal can be directly related to impulse response of a mobile radio channel. Mobile radio channel can be modeled as a linear filter with a time varying/unvarying impulse response [21]. The time varying impulse response is introduced by the moving transmitter or receiver or the intermediate objects.
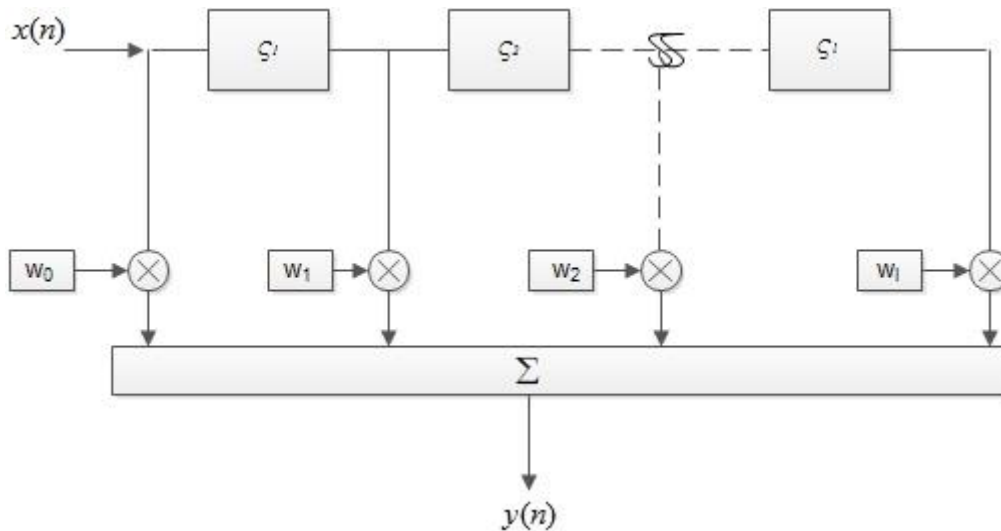
Figure 3.2: Tapped delay line implemented using l number of delayed element and-changing/constant weight.

A wideband fading model can be implemented using number of taps and coefficients where each tap represents respective multipath component or a line of sight component based on delay unit. In *Figure 3.2*, input signal $x(n)$ is passed through the linear filter to generate an output signal $y(n)$ which can be expressed as

$$y(n) = \sum_{k=0}^{L} W_k \, x \left(n - \tau_k \right)$$

(3.2)

Where $\tau_0 = 0$ represents the tap for the line of sight component whereas remaining tap delay (τ_1 to τ_l) represents the multipath component as a delay unit.

3.2   Existing Implementation of SI Channel Model

Rician channel are stochastic model for radio propagation. It assumes that the signal arrives at the receiver through various multipath including one line of sight component. Rician "K" parameter determines how strong the line of sight component is with respect to other reflective component. In this section, we will discuss about the SI channel modeling used in the literature [4,18].

In [4], omnidirectional antenna has been assumed for both transmitter and receiver. These antennas have been place quite near to each other which receives high power from line of sight and low power from other reflected component. This models channel as a Rician channel. SI channel is the channel between transmitting and receiving antennas that are close to each other [8]. This results in the high K- factor because of the strong line of sight component and weak scattered component. According to [22], Rician channel can be model as

$$h_i(\theta) = \frac{P_d}{2\pi(K+1)}[1+2\pi\delta(\theta-\theta_o)] \tag{3.3}$$

Where K is the ratio of specular to diffuse signal power, θ_o is the angle of arrival. P_d is received SI power. Auto covariance of the received signal is approximated as [4]

$$\rho(r) \approx exp\left[-23\frac{2K+1}{(K+1)^2}\left(1+\frac{K}{2K+1}\right)\left(\frac{r}{\lambda}\right)^2\right] \tag{3.4}$$

According to equation 3.4, the channel coherence is proportional to the auto covariance and the channel is coherent for small distance r and the large power ratio K [23]. Since transmitting and receiving antenna are closely located in the transceiver, this channel is quite useful to implement as a SI coupling channel. In other word, the received signal is highly correlated with the transmitted signal when passed through the Rician channel.

In [18] author has mentioned about the changes in "K" factor value before and after the analog cancellation. It has been assumed that the K factor is quiet high before analog cancellation because of the closer proximity of transmitting and receiving antenna with a strong line of sight component. But after the active cancellation, strong LOS component is reduced. This means after analog cancellation magnitude of SI signal is Rician distributed with a low "K" factor.

In [18], author has measured Kullback Leibler (KL) distances between the histogram of channel estimate magnitudes obtained from experiments and probability density function of a Rician and Rayleigh distribution. The K factor for Rician distribution was computed from the experiment whereas the K factor for Rayleigh was fixed to 0. The author observed the KL distances were lower for Rician than Rayleigh and concluded that Rician distribution was suitable for SI channel modeling.

3.3   Implementation of SI Channel in LabVIEW

We have assumed a frequency selective Rician channel as a model for self-interference channel. Even though the Doppler spread can be considered ideally 0 in the presence of stationary transmitter and receiver, LabVIEW's Rician function defines the interval for the Doppler spread as [24]

$$\frac{doppler\ spread}{sampling\ rate} = [1E\text{-}6\,,0.5] \tag{3.5}$$

So, a minimum Doppler spread was chosen so as to make the channel slowly time varying as possible and also fulfills the criteria given by equation 3.5. LabVIEW's function "*Rician fading profile*" generates multipath fading profile and "*apply selective fading profile*" applies multipath fading profile to input complex waveform for each path. Each function is discussed in detail below.

- *Rician fading profile*

    A Rayleigh distribution was generated for each path using Jake's model. Jakes fading model is a deterministic method for generating a Rayleigh fading waveforms. It assumes that N equal strength rays for each path arrives at a moving receiver with uniformly distributed angle of arrival α_n as shown in *Figure 3.3*. Each individual ray experiences a Doppler shift defined as [25]

$$\omega_n = \omega_m \cos(\alpha_n) \tag{3.6}$$

$$\omega_m = 2\pi f v / c \tag{3.7}$$

Where ω_m is the maximum Doppler shift, f is a carrier frequency, v is the vehicle speed, c is the speed of light and α_n is an angle of arrival. As seen from *Figure 3.3*, there is a symmetricity in the magnitude of Doppler shift except for angles 0 and π. Thus the waveform can be generated with $N_0 + 1$ complex oscillators with total number of rays N arriving at a node, where N_0 is defined as [25]

$$N_0 = \left(\frac{N}{4} - \frac{1}{2} \right) \tag{3.8}$$

Multiple uncorrelated waveform as a function of time (t) is generated using the equation given below [25].

$$T(t, j) = \sqrt{2/N_0} \sum_{n=1}^{N_0} A_j(n) \left\{ \left[\cos(\beta_n) + I \sin(\beta_n) \right] \cos(\omega_n t + \theta_n) \right\} \tag{3.9}$$

Where j is the path index and $\beta_n = \pi n / N_0$ for n = 1 to N_0. $A_j(n)$ is the jth Walsh Hadamard code sequence which produces ± 1 values and ensures the uncorrelated waveforms for different path. The oscillator phases, θ_n are generally randomized and are insensitive to correlation properties.

The waveform for each path can be generated using equation 3.9. Rician distribution can be generated just by adding amplitude contribution by LOS component defined by the K parameter to the first path whereas the remaining paths are Rayleigh distributed.
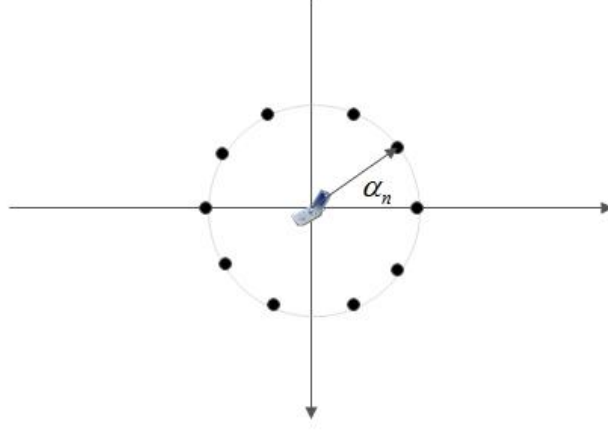
Figure 3.3: N=10 different rays arriving at a moving receiver with an angle of arri-val α_n .

- *Apply selective fading profile*

  In order to match the output complex waveform power from the channel to the specified fading variance, this LabVIEW function first normalizes the power array of the power delay profile defined as [24]

$$\bar{C}_k^2 = \frac{C_k^2}{\left(K_{LOS}+1\right)\times C_1^2 + \sum_{k=2}^{N} C_k^2} \tag{3.10}$$

$$C_k^2 = 10^{P_k/10} \tag{3.11}$$

where k is the path index from 1 to N different path. K_{LOS} is the K parameter in linear scale. P_k and C_k is the power defined for each path by the power delay profile in linear and logarithmic scale respectively.

These normalized power coefficients given by equation 3.10 are then multiplied with the fading waveform generated by the LabVIEW function "*Rician fading profile*" as defined by equation 3.9. The resultant product is defined as [24]

$$a_{kl} = \bar{C}_k \times T_{kl} \tag{3.12}$$

where $k = 1$ to N is the path index and $l = 1$ to L, where L is known as profile length and is generally equal to the length of input signal samples applied to the Rician channel. T_{kl} is the fading waveform defined by equation 3.9 for each path k and total number of fading samples L. The input complex waveform are then delayed by τ_k whose delays are define by the power delay profile. The delay τ_k is approximated to integer multiple of sampling time defined as

$$n_k = \frac{\tau_k}{dt} \tag{3.13}$$

The delayed input samples $x[n]$ are then multiplied with the fading amplitude a_{kl} point by point, using tapped delay line .The output waveform from the channel can be expressed as [24]

$$y[n] = \sum_{k=1}^{N} a_{kl}\, x[n - n_k]$$

(3.14)

An experiment was conducted in LabVIEW for three different path with power delay profile and channel parameter shown in table below.

Table 3.1: Power Delay Profile

Delay (sec) τ_k	Relative Power(dB) P_k
0	0
1.25E-8	20
2.5E-8	30

Table 3.2:Channel Parameters

Parameters	Specification
Number of Path	3
Sampling Time(dt)	1.25E-8sec
Fading Variance	1
Doppler Spread	80Hz
K	35.8 dB

In *Figure 3.4*, response for three different path is plotted against sampling interval for 80Hz Doppler spread. It can be seen, the response for the Line of sight component is similar for all sampling interval whereas the remaining path is varying slowly with the time. As shown in *Figure 3.5*, increasing the Doppler shift to 20 KHz can significantly increases the rate of change of response for each path.

Figure 3.4: Normalized Fading Response generated for three different path with the specification listed in table 3.1 and table 3.2 with Doppler spread of 80 Hz.
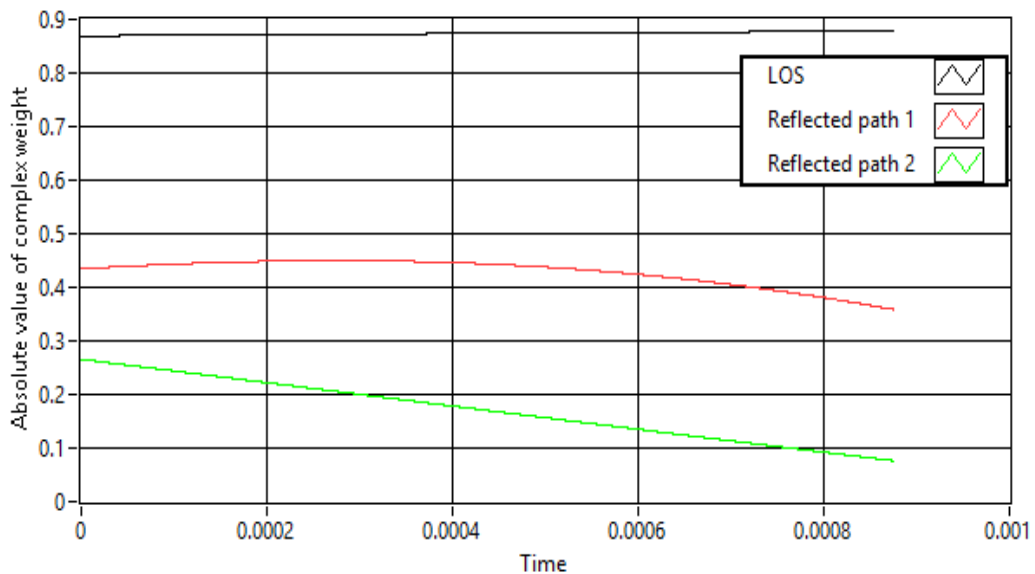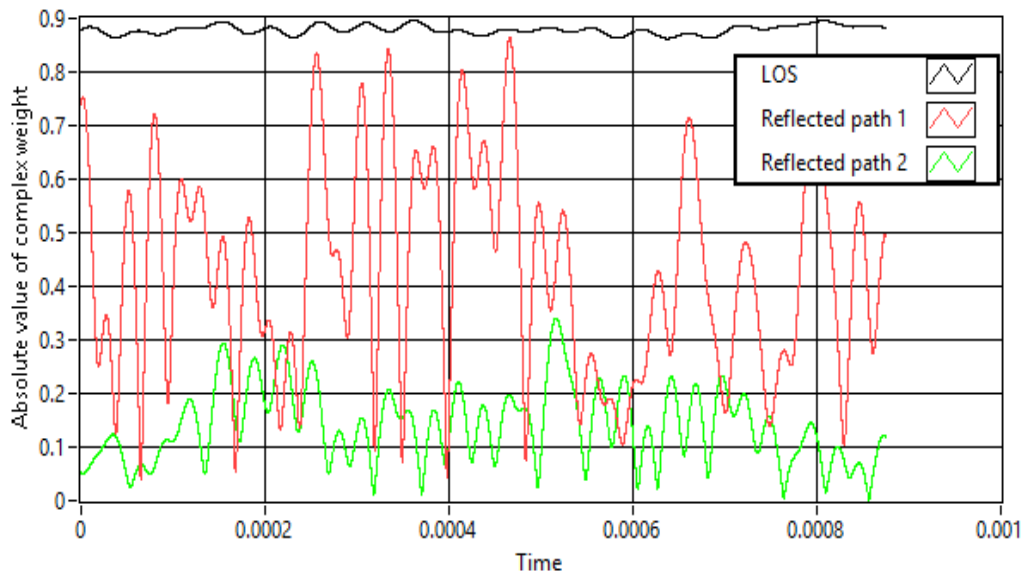
Figure 3.5: Normalized Fading Response generated for three different path with the specification listed in table 3.1 and table 3.2 with Doppler spread of 20 KHz.
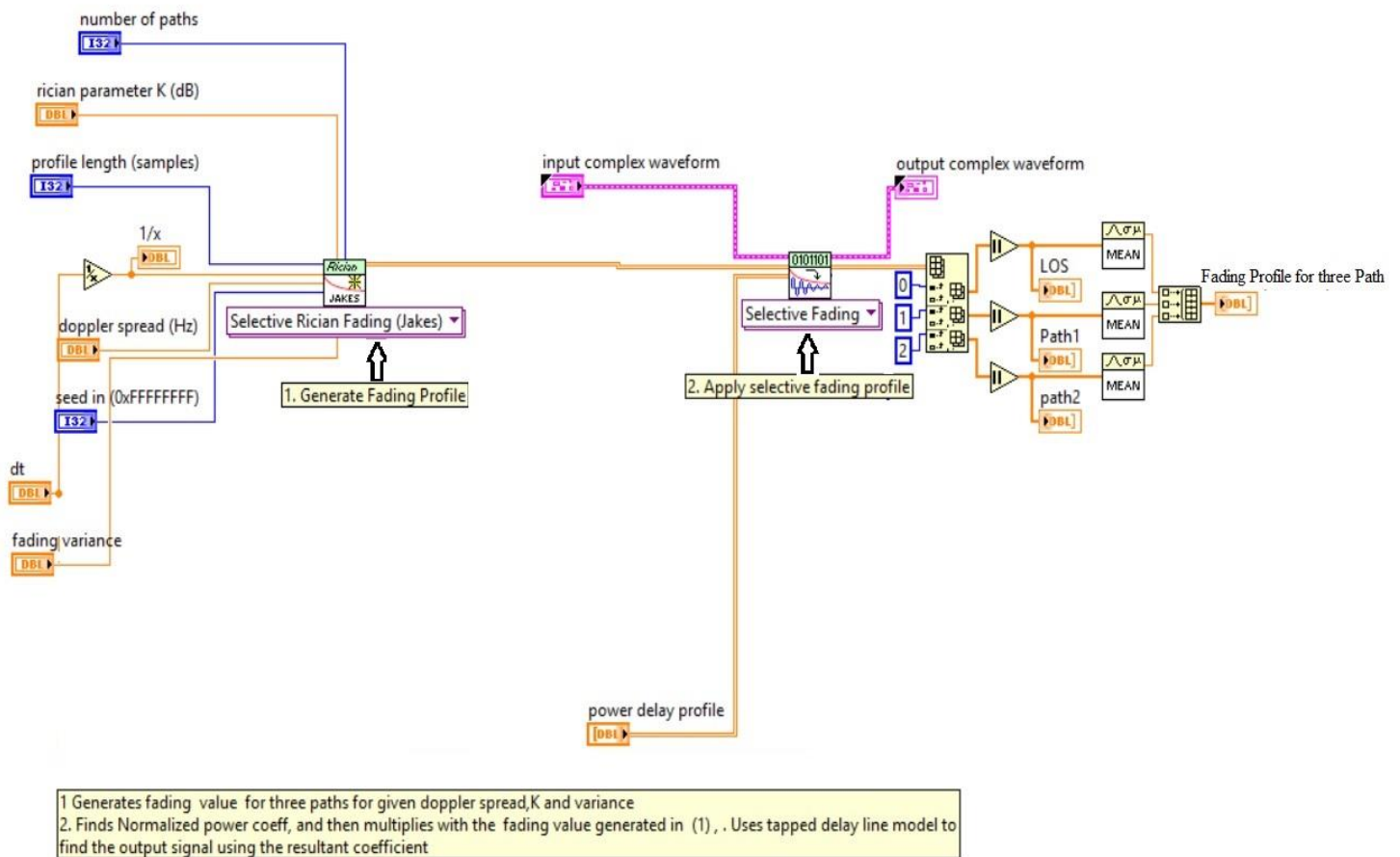

Figure 3.6: A LabVIEW code implementation of Rician Channel using library function Generate fading profile and Apply selective fading profile.

In *Figure 3.6*, interconnection of two functions *generate fading profile* and *apply selective fading profile* has been depicted. *Generate fading profile* uses number of parameters which is listed and explained below

- Number of paths
  This parameter specifies the number of paths in the simulated multipath channel. A fading profile is generated for each path.
- Rician Parameter K
  This parameter specifies K value of channel in dB scale. A large positive value of K indicates a strong additive white Gaussian noise channel whereas a large negative value indicates a Rayleigh fading.
- Profile Length
  This specifies the length of the complex valued fading profile samples (coefficients) to generate.
- Doppler Spread
  This specifies the desired input Doppler spread of channel. The Doppler spread cannot be taken 0 and should fall within a range define by equation 3.5. The unit of Doppler spread should be in Hz.
- Fading variance
  This specifies the desired variance of complex valued fading profile. During the experiment this value was not changed and kept constant to 1.
- dt
  It specifies the sampling time of system and is expressed in seconds.
- Fading Profile
  It returns complex valued coefficients. The number of rows corresponds to the number of paths in channel and the number of columns is equal to the profile length. This fading profile is then applied to the Rician function *apply fading profile*.

The parameter used in *apply fading profile* function is listed and explained below.

- Input Complex Waveform
  It specifies the input modulated complex baseband waveform data. This waveform signal should also contain the sampling time of the signal.
- Fading profile
  It a 2 dimensional input which is fed from the output *of generate fading profile* function. The coefficients generated by *generate fading profile* is applied sample by sample to the input complex waveform.
- Power delay profile
  It specifies the arrival time of different ray paths in seconds versus their respective power in dB. The times are relative to arrival of the first ray path and the power must be relative power loss.

- Output complex waveform

  It returns the Rician faded complex baseband waveform data. The length of the output complex waveform is equal to the length of input complex waveform regardless the size of fading profile. The size of fading profile is specified by profile length.

- Fading Profile for three path

  This is not a library function output but still this function has been modified to view the normalize coefficients of the channel as explained in equation 3.10 to 3.12. LabVIEW uses these normalized coefficients as a weight of SI channel to convolve with input signal rather than fading profile.

4   Adaptive Digital Self Interference Cancellation

Adaptive filter has the ability to change its parameter automatically unlike conventional filters. The filtering process is adaptive thus does not need any prior information regarding signal or noise characteristic. However, the noise component in the corrupted signal and noise signal in the reference channel should be highly coherent in order to cancel out the noisy component [3].

In this chapter we will discuss on the background of LMS algorithm, formulate LMS algorithm for SI cancellation and finally discuss on the implementation of LMS algorithm in LabVIEW.

4.1 Background on LMS Algorithm

Least Mean Square is a linear adaptive filtering algorithm which computes the output of a filter in response to an input signal. The LMS algorithm is a member of stochastic gradient algorithm which operates on stochastic inputs. An estimation error is calculated by taking the difference between filtered output and the desired signal. The weight of filter is adjusted by using this estimated error. The filter weight is updated until the mean square error is minimized.
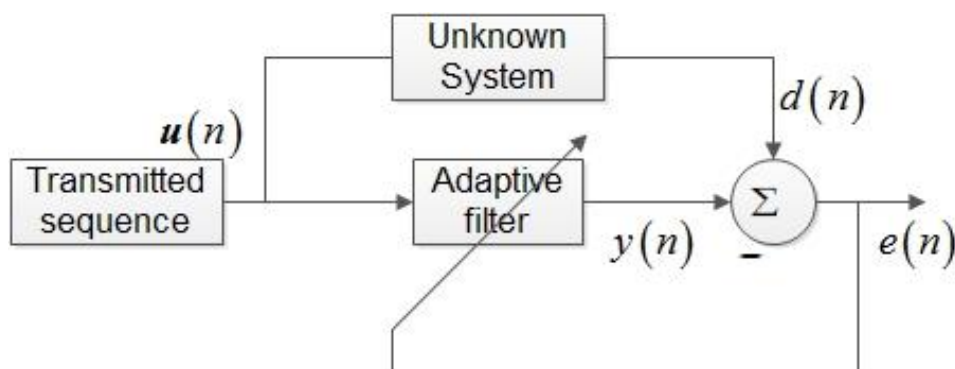
Figure 4.1:An adaptive filtering for system identification.

A transversal filter is built along with LMS algorithm which is used for the filtering process. An adaptive algorithm like LMS is used to perform the adaptive control process on the taps of the filter. The step size μ which controls the convergence rate of algorithm depends on the maximum value of PSD of tap inputs $u(n)$ and filter length M which can be represented as following inequality [10]

$$0 < \mu < \frac{2}{M \, S_{max}} \qquad (4.1)$$

Where S_{max} is the maximum value of the PSD of the tap inputs $u(n)$. The step size μ should be chosen carefully. The large amount of μ might change the weight of the adaptive filter by large value due to which instead of converging the error, it might start to diverge. The upper bound for the step size is given by inequality (4.1). In *Figure 4.1* , transmitted sequence $u(n)$ is generated and passed through a unknown system to generate signal $d(n)$. The signal $u(n)$ is also passed through an adaptive filter. The LMS algorithm updates the weight of adaptive filter in each iteration by equation given below

$$y(n) = \hat{w}^{H}(n)u(n) \tag{4.2}$$

$$e(n) = d(n) - y(n) \tag{4.3}$$

$$\hat{w}(n+1) = \hat{w}(n) + \mu u(n) e^{*}(n) \tag{4.4}$$

The equation (4.2) to (4.4) is the complex form of LMS algorithm. At each iteration, this algorithm needs the most recent values of $u(n)$, $e(n)$ and $d(n)$. These new values are used to calculate the new weight $\hat{w}(n+1)$ of adaptive filter, which is also passed to the next iteration to calculate the next weight. It can be seen that the weight updating process is completely closed loop process, in which initial guess for the weight $\hat{w}(n)$ has to be made.

When the iteration is started for first time, initial weight can be almost chosen close to final weight. This could help increasing the converging rate of algorithm. In case of no prior information of weight are provided, initial weights can be assumed to be 0. In *Figure 4.1*, as the filtered signal $y(n)$ approaches close to desired signal $d(n)$, error signal $e(n)$ converges to 0. At this instant, weight is said to be completely updated and need not to be updated anymore. But if somehow the unknown system parameter changes, error signal starts to diverge away from 0, and there is requirement for weight update.

4.2 Canonical LMS Algorithm

Canonical form of LMS algorithm is quite useful when dealing with the adaptive equalization of a communication system for the transmission of a binary signal over a dispersive channel [10]. Since digital SI cancellation is done at baseband level which consists of complex symbols modulated using QPSK or QAM constellation, for which these type of algorithm are very useful which deals with real value processing of complex signal.
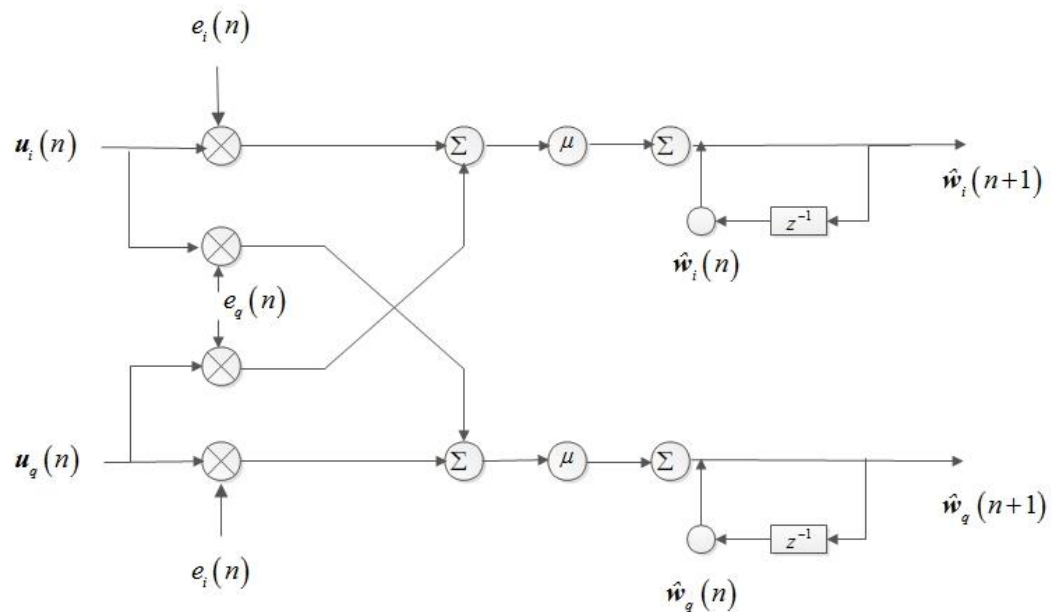
Figure 4.2:Signal flow while updating the LMS equation.

Each signal from equation 4.2 to 4.4 can be represented in complex form as shown below

$$a(n) = a_i(n) + ja_q(n)$$ (4.5)

where $a \varepsilon \{u, y, e, w\}$.

The subscript i and q denotes in phase and quadrature component, that is real and imaginary parts of signal respectively. Thus equation 4.2 to equation 4.4 can be define as

$$y_i(n) = \hat{w}_i^T(n)u_i(n) - \hat{w}_q^T(n)u_q(n)$$ (4.6)

$$y_q(n) = \hat{w}_i^T(n)u_q(n) + \hat{w}_q^T(n)u_i(n)$$ (4.7)

$$e_i(n) = d_i(n) - y_i(n)$$ (4.8)

$$e_q(n) = d_q(n) - y_q(n)$$ (4.9)

$$\hat{w}_i(n+1) = \hat{w}_i(n) + \mu[e_i(n)u_i(n) - e_q(n)u_q(n)]$$ (4.10)

$$\hat{w}_q(n+1) = \hat{w}_q(n) + \mu[e_i(n)u_q(n) + e_q(n)u_i(n)]$$ (4.11)

It can be seen from equation (4.6) to equation (4.11) and from *Figure 4.2*, that to implement real value processing of complex LMS algorithm, set of four real LMS algorithm with cross coupling between them is required.

This type of equalizer is placed in the receiver chain where the output of the channel is used as the input signal. Its parameters are then adjusted using LMS algorithm to provide estimation to each symbol transmitted. During the training mode, a copy of desired response is stored in the receiver. This training sequence has to be synchronized with the transmitted sequence which is generated using PN sequence generator. PN sequence uses number of feedback shift registers that produces the deterministic waveform periodically. Once the parameters for the transversal filter are estimated, data transmission can begin [10].

4.3   LMS Algorithm in SI Cancellation

Let vector x_n be the original baseband transmit signal passed through the self-interference channel. The multipath SI channel between the transmitting and receiving antenna is modeled by an FIR filter whose impulse responses are generated using Rician distribution as explained in section 3.3 and is denoted as h_n .
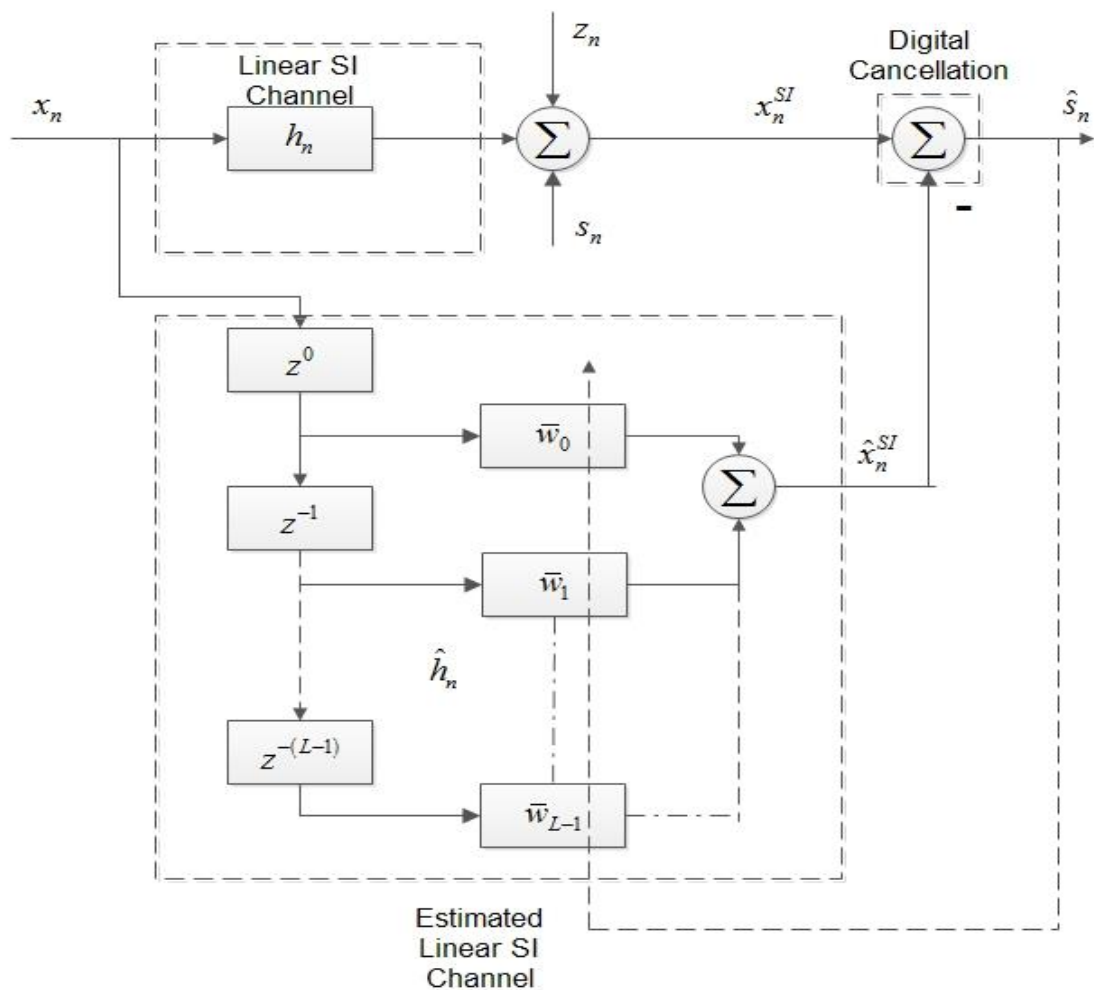

Figure 4.3: Baseband transceiver modeling and LMS canceller structure.

Let us define vector $\bar{w}_n = [\bar{w}_0, \bar{w}_1, \ldots, \bar{w}_{L-1}]$ as a coefficient of the estimated channel and vector $w_n = [w_0, w_1, \ldots, w_{L-1}]$ as the coefficient of the SI channel. Thus the total received signal before digital cancellation is defined as

$$x_n^{SI} = \sum_{k=0}^{L-1} w_k x_{n-k} + z_n + s_n \tag{4.12}$$

where z_n and s_n are additive Gaussian noise and signal of interest respectively.

The self-interference estimated channel output having response of $\hat{h}_n$, is given as

$$\begin{aligned}\hat{x}_n^{SI} &= x_n \otimes \hat{h}_n \\ &= \sum_{k=0}^{L-1} \bar{w}_k\, x_{n-k}\end{aligned} \tag{4.13}$$

As seen from *Figure 4.3,* the output of digital canceller $\hat{s}_n$ which can be consider as error signal in the context of LMS algorithm is defined as

$$\hat{s}_n = x_n^{SI} - \hat{x}_n^{SI} \tag{4.14}$$

Since the main objective of the digital cancellation in this thesis is the ability to automatically adapt to the coefficient of the SI channel. Thus applying all the available parameters to define the equations provided by the LMS algorithm we can write with reference from equation 4.4,

$$\bar{w}(n+1) = \bar{w}(n) + \mu x_n(n)\hat{s}_n^* \tag{4.15}$$

The equation 4.15 gives iterative process of updating the weight of the estimated channel. The right most term $\mu x_n(n)\hat{s}_n^*$ has to be 0 for the present weight $\bar{w}(n)$ and the next weight $\bar{w}(n+1)$ to be equal. Since the step size μ is always greater than 0, the updated weight $\bar{w}(n+1)$ and the present weight $\bar{w}(n)$ can be equal only if the error term $\hat{s}_n^*$ becomes equal to 0. For $\hat{s}_n^*$ to be 0, the term x_n^{SI} and $\hat{x}_n^{SI}$ should be equal which can only happen if the estimated weight $\bar{w}_n$ becomes equal to the SI channel weight w_n. Since the total received signal consist of noise z_n and the signal of interest s_n, the output of digital cancellation after complete SI cancellation can be can be written as

$$\hat{s}_n \approx z_n + s_n \tag{4.16}$$

The autocorrelation matrix of the tap input vector x_n can be expressed as

$$R = E[x_n(n)\, x_n^H(n)] \tag{4.17}$$

Thus the condition for stability of adaptive filter can be expressed with inequality as[10]

$$0 < \mu < \frac{2}{\lambda_{max}} \tag{4.18}$$

where λ_{max} is the maximum Eigen value of autocorrelation matrix $\boldsymbol{R}$.

According to equation 4.18, the range of step size is controlled by the Eigen value of auto correlation matrix.

4.4 Design of LMS Algorithm in LabVIEW

A buffer was deigned to store the input samples. The size of buffer was made equal to the length of the filter. An initial weight of the adaptive filter and the initial buffer was assumed to be zero. The process of weight update is shown in the *Figure 4.4*.
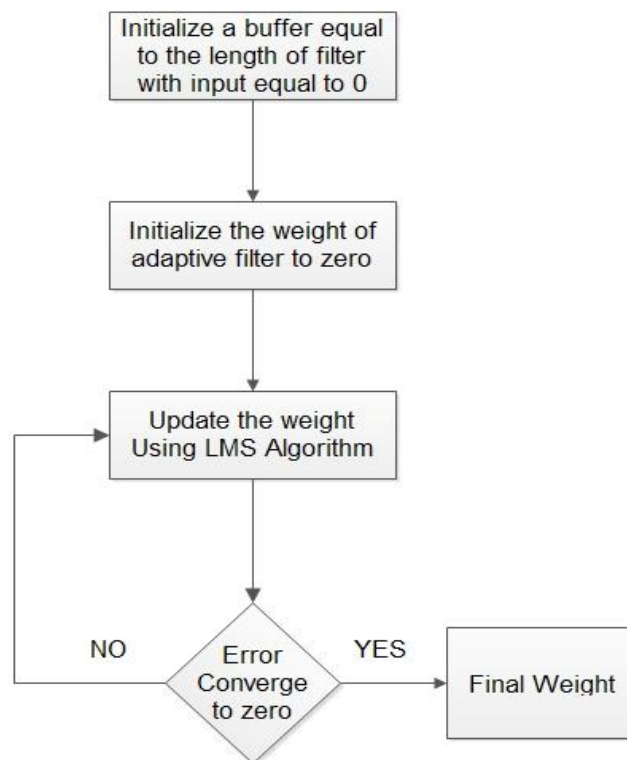
Figure 4.4:A flowchart showing steps to update the weight of filter.

In each iteration a new sample was added to the buffer and the last sample was discarded. In each iteration, buffered input samples were filtered using the updated weight until all the input samples were filtered out. It is important to note that the input samples should be long enough to calculate the optimal weight so that the error signal converges to 0. The whole program code is divided into three different stages known as *creating array of input signal*, *filtering stage* and *weight update stage* as shown in the *Figure 4.9* (starting from bottom to top).

- *Creating Array of Input Signal*

This stage refers to the stage where all the input samples are stored in a buffer. The LabVIEW function "*build array*" (shown as 1 in the code depicted in *Figure 4.5*) inserts one new sample in every iteration to the buffer. The new sample inserted is placed at the last index of the buffer. "*Rotates 1D array*" (shown as 2 in the code depicted in *Figure 4.5*) shifts the element to the left once such that the element in the first index comes to last index when the rotation index is initialized with constant -1.

1 Build array: Inserts new element(one sample) in each iteration to form an array. result length of array is always equal to L+1 New element is always inserted at last index

2. It rotates the array given by (1) to the left only once such that element in the first index comes at last index
3. it truncates the size of array to L and kicks off the element at last index forming array for input signal x(n)
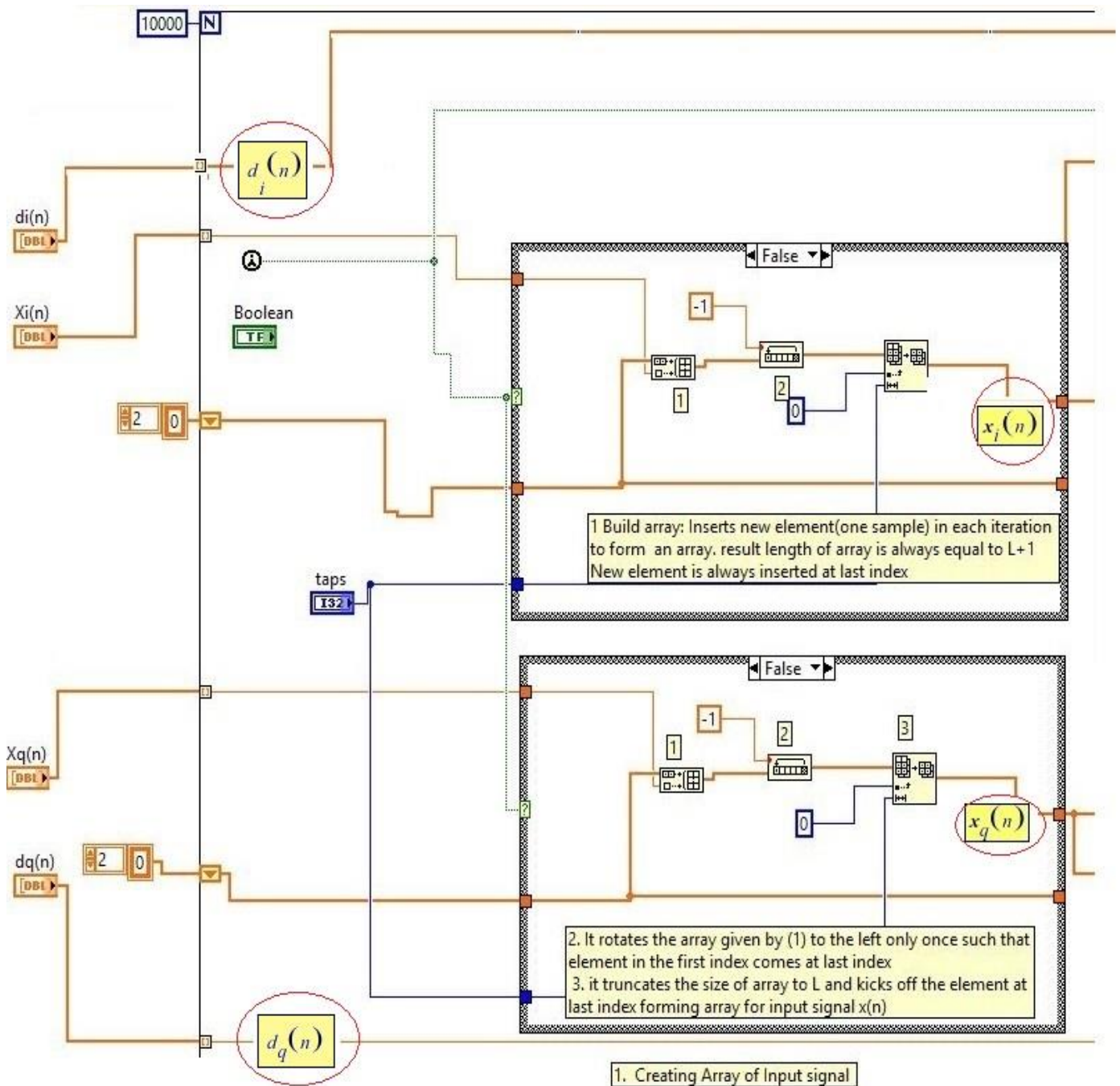
1. Creating Array of Input signal

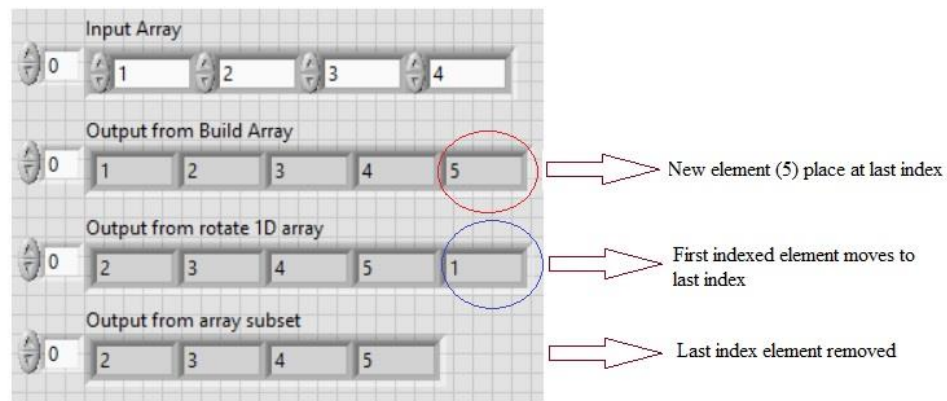*Figure 4.5:Buffering stage implemented in LabVIEW platform*

Figure 4.6: An example explaining each functions of buffering stage.

The function "*array subset*" (shown as 3 in the code depicted in *Figure 4.5*) removes off sample at last index so as to make the length of buffer always constant. Initially all the input samples of buffer is initialized to 0. In *Figure 4.5,* the in phase and quadrature component of input signal is denoted as $x_i(n)$ and $x_q(n)$ respectively. The signal $x_i(n)$ and $x_q(n)$ is consider as real and imaginary component of baseband signal x_n with reference to *Figure 4.3*. The desire response $d_i(n)$ and $d_q(n)$ are the desired response and is consider as output of SI channel x_n^{SI} with reference to *Figure 4.3*.

In *Figure 4.6*, an example of buffering stage has been explained. It can be seen that the buffering stage stores a sample and shifts element in every iteration. During the shifting process, the oldest sample in the buffer is removed. The size of buffer is made equal to number of taps of estimation filter.

- *Filtering Stage*

  The next stage is referred as filtering stage in which complex weight of filter is divided into real and imaginary component $w_i(n)$ and $w_q(n)$ respectively and is multiplied with respective real and imaginary component of input signal as explained in equation 4.10 and 4.11 to get filtered signal $y_i(n)$ and $y_q(n)$ as shown in *Figure 4.7*.

  The filtered signal $y_i(n)$ and $y_q(n)$ is consider as the real and imaginary component of $\hat{x}_n^{SI}$ with reference to *Figure 4.3*. The addition and the multiplication function is placed inside for loop, due to which arithmetic operation takes place sample by sample. Initially the weight of the filter has been initialized to 0 through feedback node. All the input signal and output signal are placed on top of the wire

and inside red circle in *Figure 4.7*. The weight signal $w_i(n+1)$ and $w_q(n+1)$ are real and imaginary component of weight $w(n+1)$.
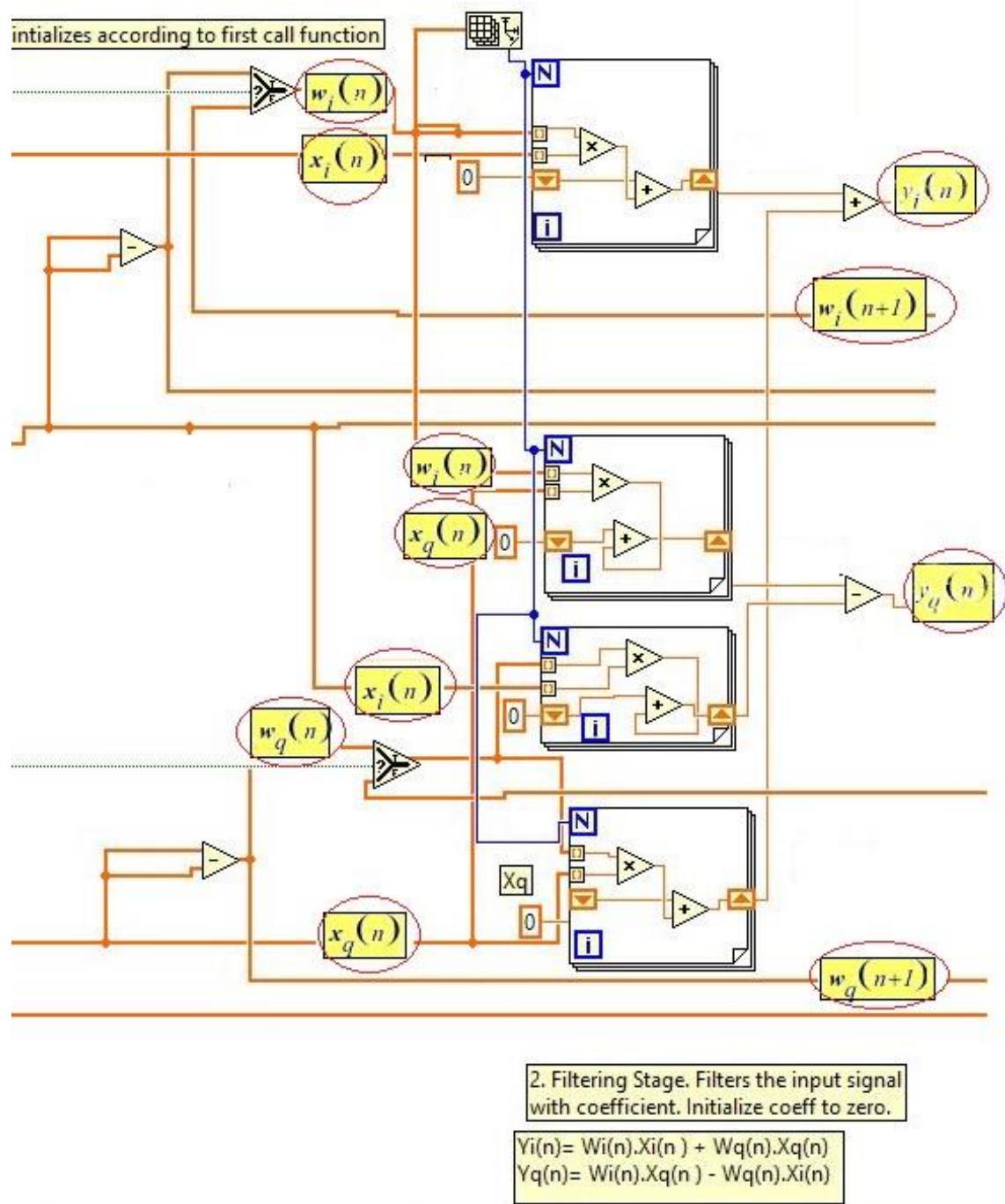
Figure 4.7:A LabVIEW design of filtering stage.

- *Weight Update stage*

This is the final stage where we apply LMS algorithm to update the weight in each iteration. *Figure 4.8* depicts weight updating stage.
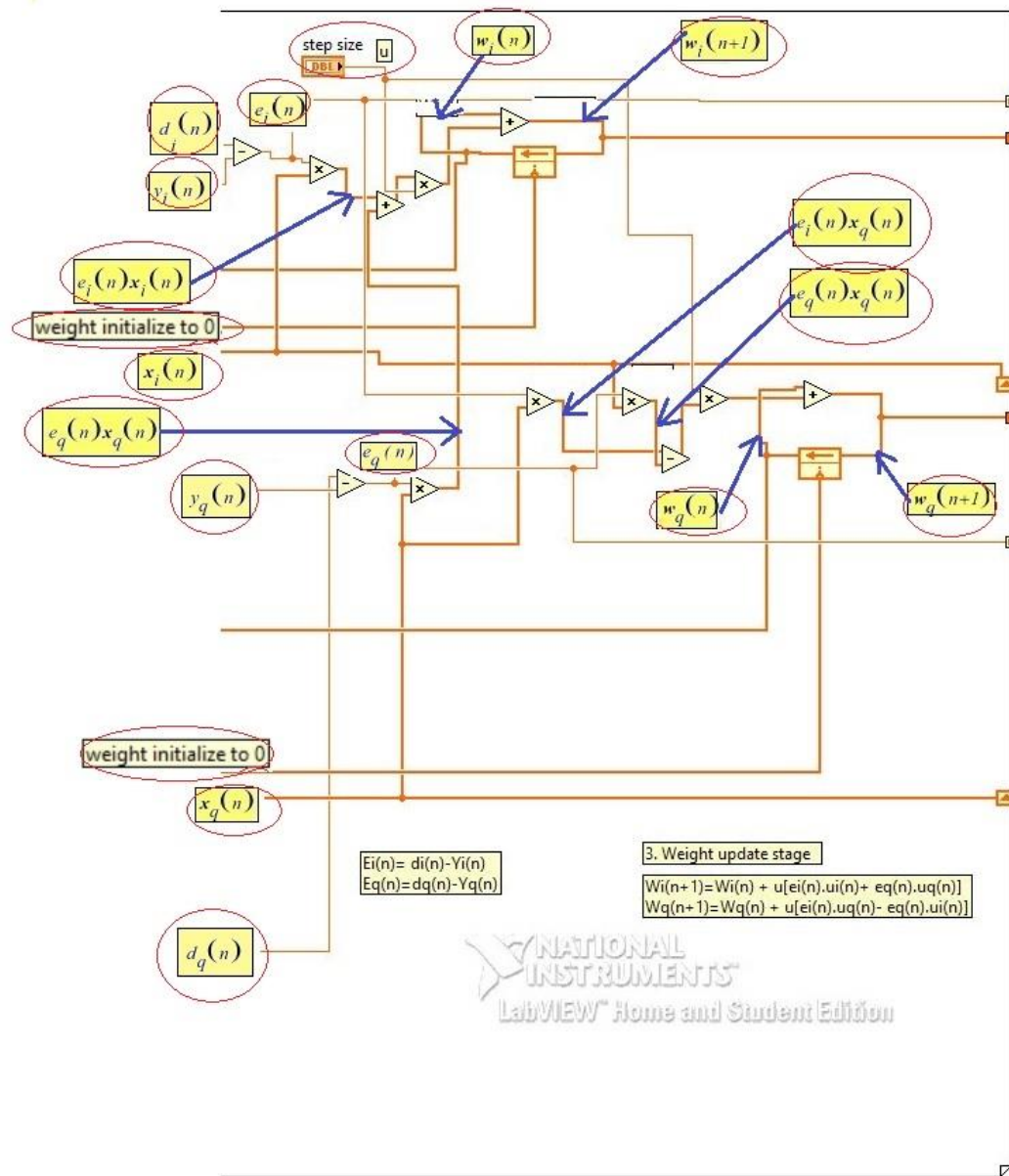
Figure 4.8: A LabVIEW design of weight update stage.

The desired signal $d(n)$ and the filtered signal $y(n)$ is subtracted to obtain the error signal. The real and imaginary component of weight $w(n)$ is calculated using equation 4.10 and 4.11. The calculated weight is consider as the weight of the estimated channel $\overline{w}(n)$, with reference to equation 4.15. Feedback node was used to pass the updated weight $w(n+1)$ to the next iteration. The input signal sample $x_i(n)$ and $x_q(n)$ are also passed using shift register function of Lab-VIEW so as to update the buffer for next iteration. The initial guess for the weight was assumed to be 0. Each input and output signal are placed on top of wire and inside red circle.

The interconnection of all three stages can be seen in *Figure 4.9.*

Figure 4.9: A LabVIEW design of canonical LMS algorithm.

5 Transceiver Model

In this thesis, we have conducted an experiment on SI cancellation using simple baseband transceiver which was implemented in LabVIEW. This chapter contains a section where general RF transceiver that was implemented in [17] for digital SI cancellation is explained. The next section contains an explanation of a baseband transceiver that was implemented in this thesis work for SI cancellation.

5.1 Full Duplex RF Transceiver

A direct conversion transceiver converts the baseband signal directly to the RF signal by using a mixer and is widely used model in mobile communication.

As shown in *Figure 5.1*, transmitted bits are encoded and passed through DAC and then filtered out with Low pass filter. This filtered signal is amplified with Variable Gain Amplifier (VGA) and power amplifier.
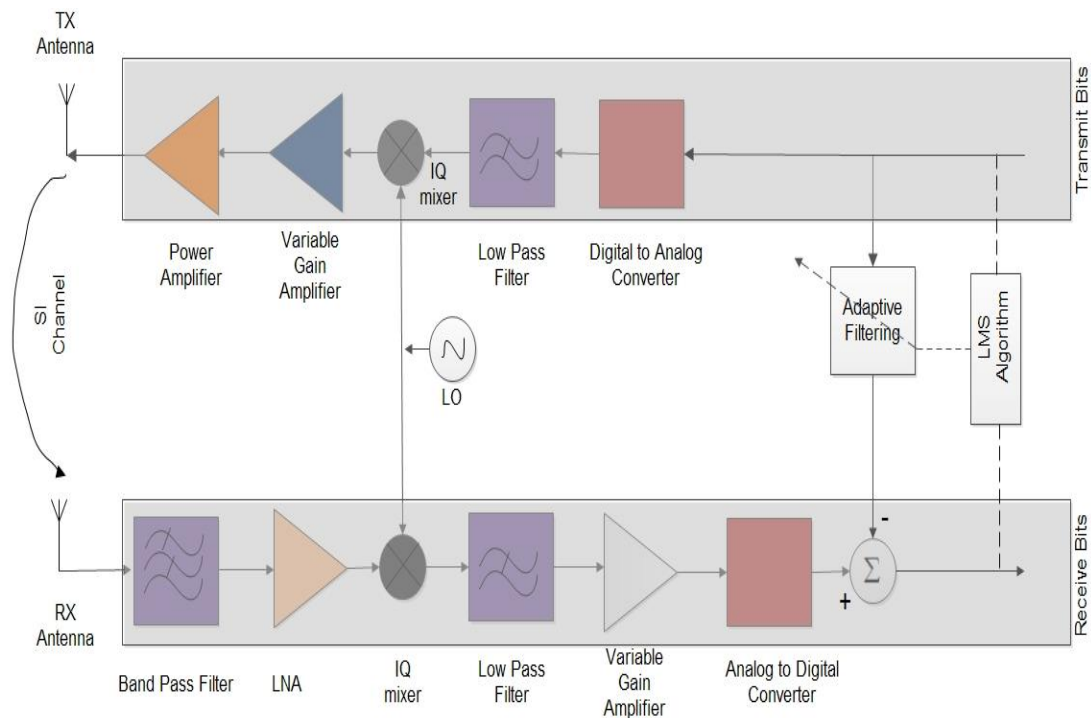

Figure 5.1: A high level block diagram of direct conversion Full Duplex Transceiver model showing digital adaptive cancelling stage in the transceiver.

At the receiving side, the received signal is passed through Band pass filter and then to LNA. Then the signal is down converted to base band signal. VGA at the receiving side control the received signal strength such that the signal falls within the dynamic range of the ADC.

The taps input for the adaptive filter were taken from the transmitter chain before DAC and the cancellation was carried at the receiver chain. The baseband cancellation samples were taken from the output of ADC of receiver chain. The error signal was generated by taking the difference of these cancellation samples and output of the adaptive filter signal.

5.2 Implementation of Baseband Transceiver in LabVIEW

This thesis focuses on the linear digital SI cancellation and thus non idealities induced by the transceiver is ignore. Moreover, no up conversion or down conversion was carried in LabVIEW because the SI cancellation was carried out at baseband. In this thesis, we have assumed a separate antenna for transmitter and receiver. The overall transceiver model in the LabVIEW experiment looks as shown in *Figure 5.2*.
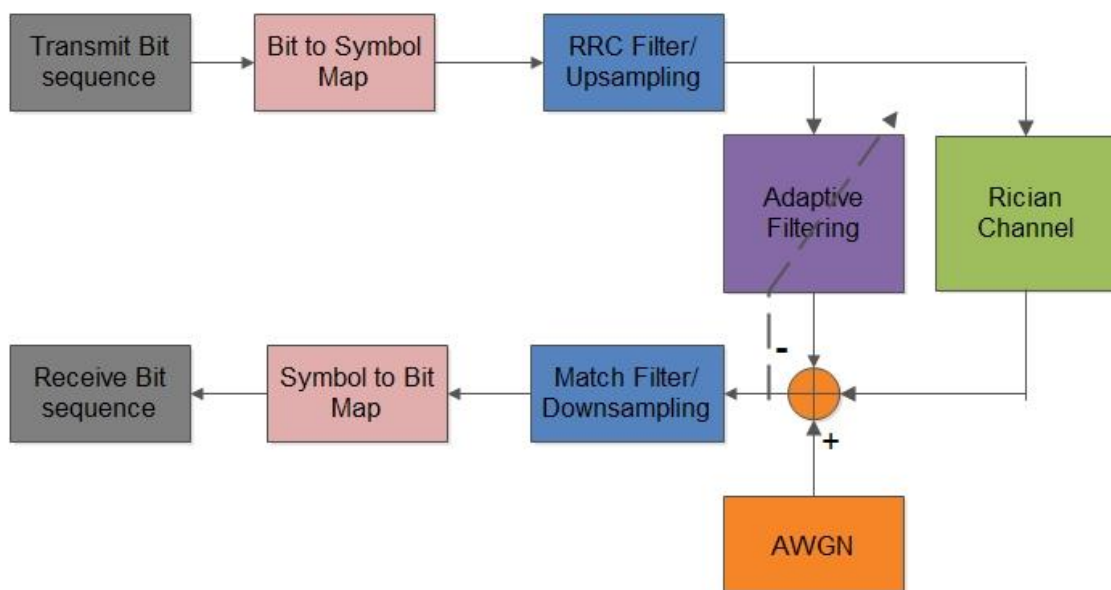

Figure 5.2: A system design layout of Full Duplex Base Band Transceiver as implemented in the LabVIEW Environment.

A pseudo random code generator was used to generate the training sequence for the adaptive filter in LabVIEW. These generated bits are then mapped into symbol with QAM constellation. These generated symbols are then passed through a pulse shaping filter and then up sampled. These generated samples were used as a tap input for adaptive filter. These samples were also fed to the input of Rician channel which was modeled as SI channel.

At the receiving end digital SI cancellation has been performed before match filtering. The samples to be cancelled were taken from the output of SI channel. The error signal is the difference of these cancellation samples and the output of the adaptive filter. LMS algorithm updates the weight iteratively using this error signal and current tap input. The digital cancellation process was done as shown in *Figure 5.2*. This thesis focuses on the amount of SI cancellation that can be achieved during the training process, rather than the actual data transmission.

6 Waveform Simulation Result and Analysis

The waveform simulation for SI cancellation has been performed with the channel parameters specified in *Table 3.1* and *Table 3.2*. The experiment has been conducted with a low Doppler spread such that channel characteristic between transmitter and receiver changes slowly with time and thus it will be easier for adaptive algorithm to estimate the SI channel parameters. The SI coupling channel between the transmitting and receiving end consist of three taps where first tap is modeled as line of sight component, remaining taps are reflected components which are delayed by one and two sample intervals as shown in *Table 3.1*. The ratio between the power of main component and the multipath component has been chosen to be 35.8 dB which is practical value for a SI coupling channel when the transceiver is located inside a room [18]. The SI channel estimation has been performed during the training period when there is no received signal of interest. In this thesis, the used figure of merit is the output power of SI digital canceller (error signal). *Table 6.1* shows the parameters for waveform simulation.

Table 6.1:Waveform Simulation Parameters

Parameter	Value
Constellation	4 QAM
Signal Bandwidth	30MHz
Symbol Rate	20MHz
Transmit Power	4 dBm
Roll off Factor	0.5
Up sampling factor	4
Number of training samples(N)	7×10^4 / varied
Number of taps of adaptive filter (M)	3/varied
Step size of LMS algorithm	0.7/ varied
E_b / N_0	50 dB
SI Channel Length	3
Noise Floor	-46.838 dBm

6.1 Learning Curve for LMS Algorithm

In *Figure 6.1* and *Figure 6.2*, real and imaginary components of error signal have been plotted. The error signal e(n), which can be referred as $\hat{s}_n$ from *Figure 4.3*, needs to be approximately equal to the sum of noise signal and signal of interest. In absence of noise

and signal of interest, error signal should be equal to 0. It can be seen from figure below, the error signal has not completely converged around 0, because a noisy signal has been added to the channel output. According to equation 4.14, error signal $\hat{s}_n$ is the difference of SI channel output x_n^{SI} and the filtered signal $\hat{x}_n^{SI}$. The noisy signal z_n and signal of interest s_n is independent of x_n^{SI}, due to which the adaptive filter will take steps in the direction of interfering signal so that external signal like noise and signal of interest are not cancelled out.
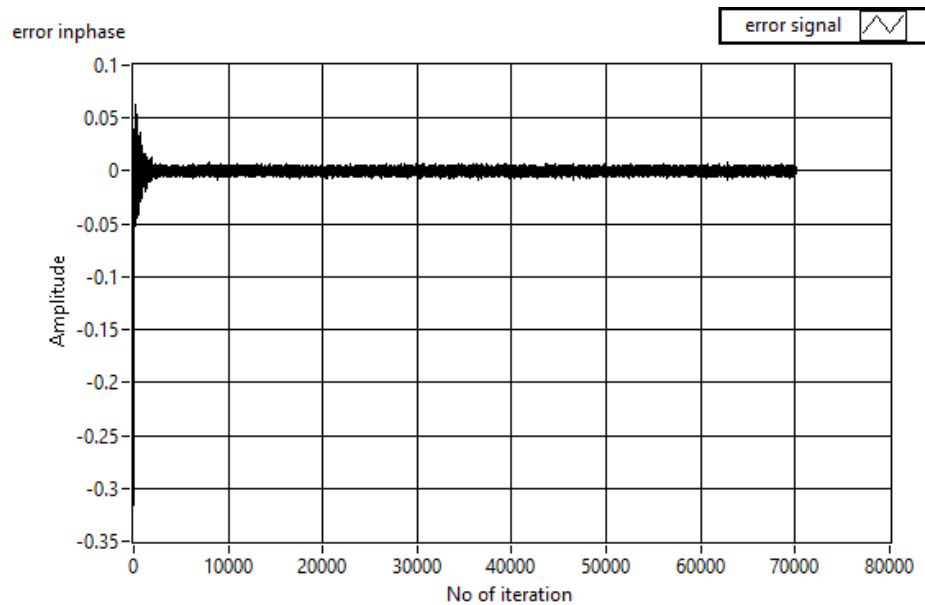

Figure 6.1: In phase Error Signal converging as the number of iteration increases
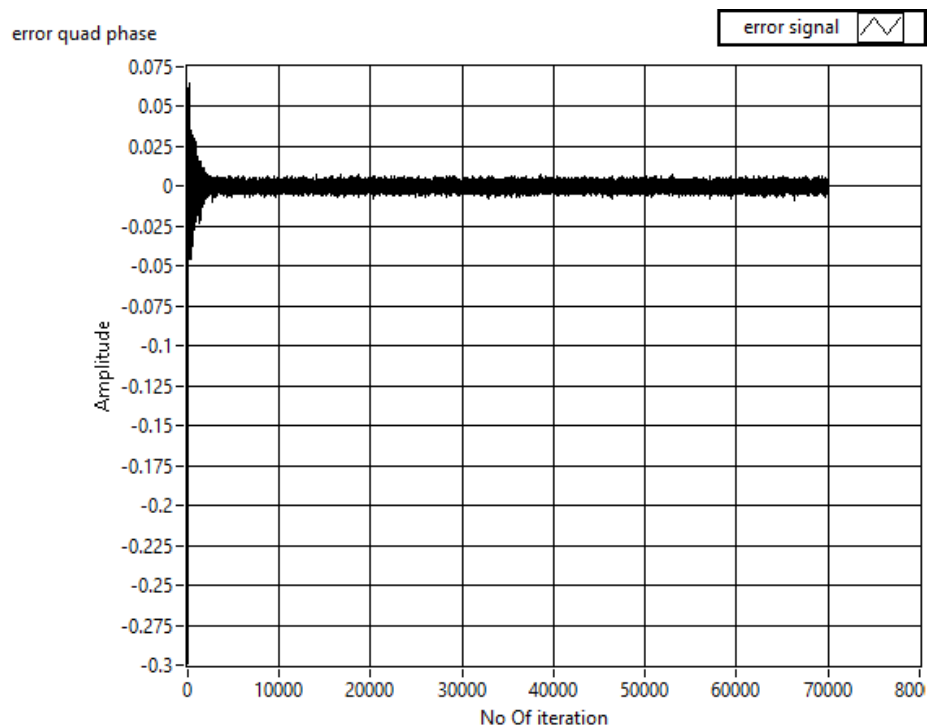

Figure 6.2: Quad phase Error Signal converging as the number of iteration increases.

It can be seen from the previous plot; the convergence of the error signal has been increased when the number of iteration has been increased.
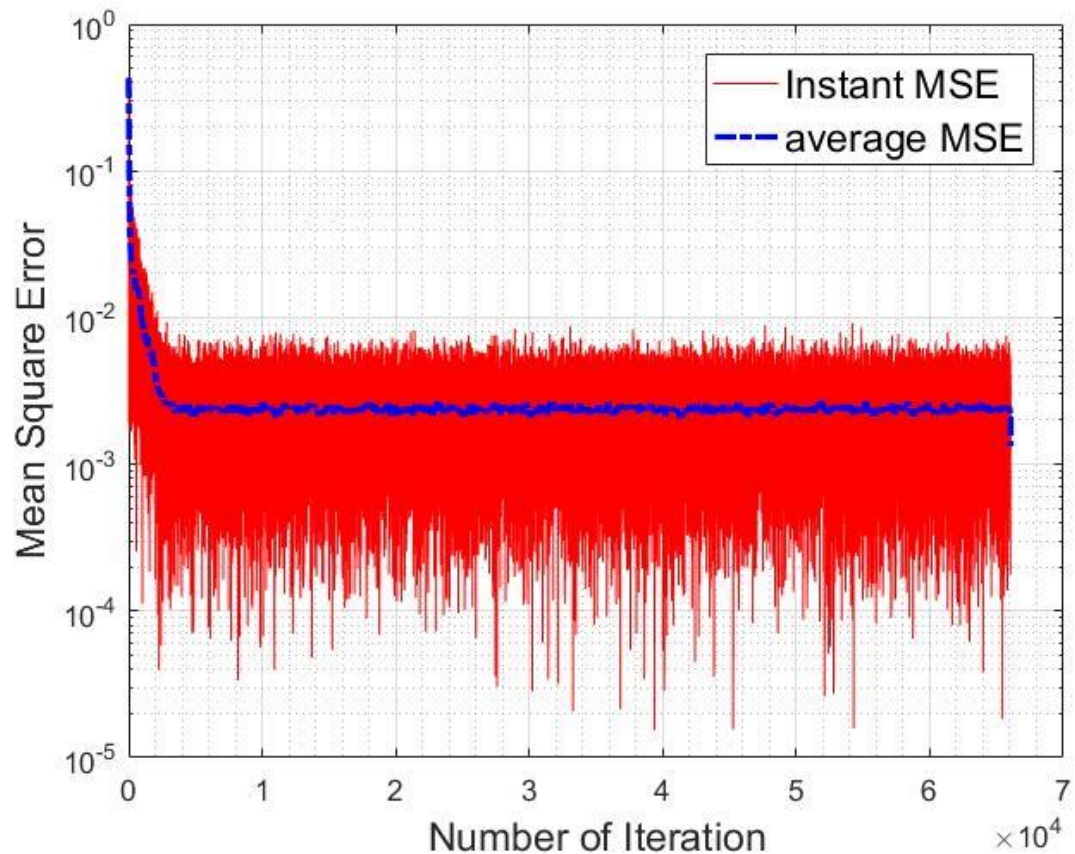

Figure 6.3: Learning curve plot for 1000 realization depicting Mean square error vs no of iteration.

A learning curve gives the better understanding performance of an adaptive filter, including convergence speed, steady state error and stability. It is calculated by taking the mean of squared error $|e(n)|^2$ over several realization of ensemble. Mathematically, it can be defined as [10]

$$J(n) = \frac{1}{K} \sum_{k=1}^{K} |e_k(n)|^2, \quad n = 0,.....,N-1 \qquad (4.19)$$

where $e_k(n)$ is the estimation error at time instant n for the $k - $ th realization, and K is the number of realization to be considered. As shown in the *Figure 6.3*, instantaneous and average MSE is plotted resulting up to 2.386×10^{-3} of estimation error. Looking at the learning curve plotted in *Figure 6.3*, we can consider that the adaptive filter starts to

converge at about 3000 iterations. The error does not reduce anymore after 3000 itera-
tions and reaches the steady state. The lesser the estimation error, the more accurately the
SI channel has been estimated.

6.2 Effect of Length of Training Sample

In the next experiment set up, the effect of length of training samples on SI attenuation
has been studied on a signal having bandwidth of 30 MHz and with step size of 0.7.

The length of training sample has been varied with steps of 5000, with minimum training
length of 500 samples to maximum of 5.5×10^4 samples in each independent run. It can
be seen from *Figure 6.4*, that the power of the digital canceller output has been decreased
with the increase in the number of training samples up to - 44.31 dBm. It should be noted
that to achieve maximum SI cancellation at least 3×10^3 samples were required.
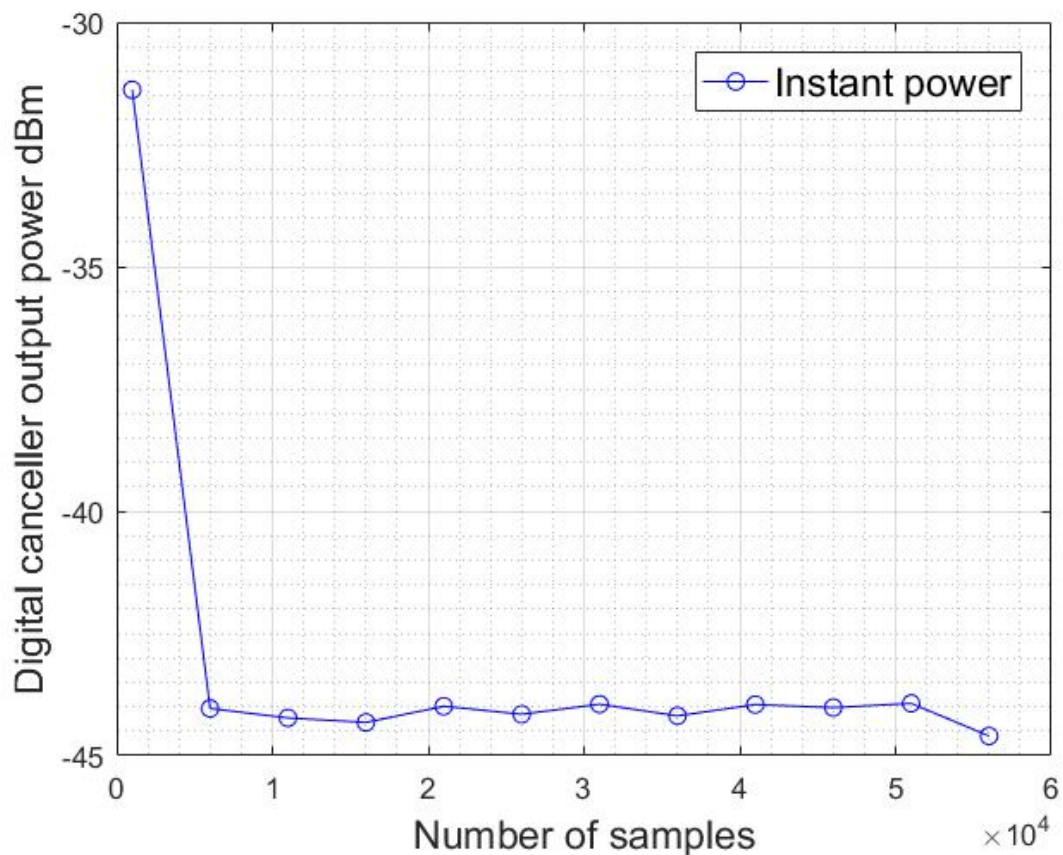

*Figure 6.4: The output power of error signal vs the amount of training samples. The
power was observed at the end of the samples with the parameters specified in the Ta-
ble 6.1.*

6.3 Effect of Step Size

In the next experiment set up, the effect of step size on the SI cancellation has been stud-
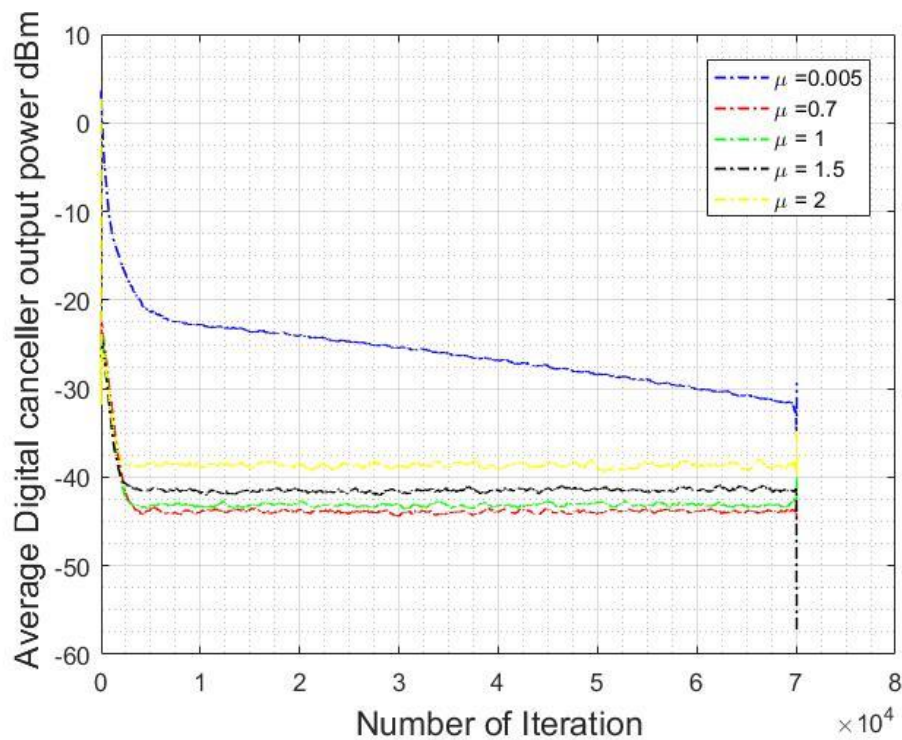ied in LabVIEW with channel parameters specified in table 3.1 and table 3.2.

Figure 6.5: The power of digital canceller output vs the number of iteration for differ-
ent step size.

The output power of SI canceller has been observed for five different step sizes. It can be
seen from *Figure 6.5*, the level of SI attenuation has been increased with the increase in
the step size for a constant number of training samples. The higher step size has resulted
in the faster convergence of algorithm. The larger step size has caused to increase the mean
square error. As seen from *Figure 6.5*, for $\mu = 1.5$ and higher, the SI attenuation starts to
decrease . This is because the step size μ should always satisfy the inequality given by
4.18. The higher step size increases estimation error of the algorithm. There is no signifi-
cant difference in the output power of digital canceller for $\mu = 0.7$ and $\mu = 1$. This means
that the SI attenuation doesn't increase beyond a certain value of step size. The minimum
digital canceller output power has been observed to be about -43.41dBm.

6.4 Effect of Signal Bandwidth

In this next set up, effect of bandwidth on the digital SI cancellation has been studied. The bandwidth of the signal has been decreased to 30 KHz. The multipath channel has been modeled as one line of sight component and two reflected components which were delayed by one and two sample interval for both narrow band and wide band signal.
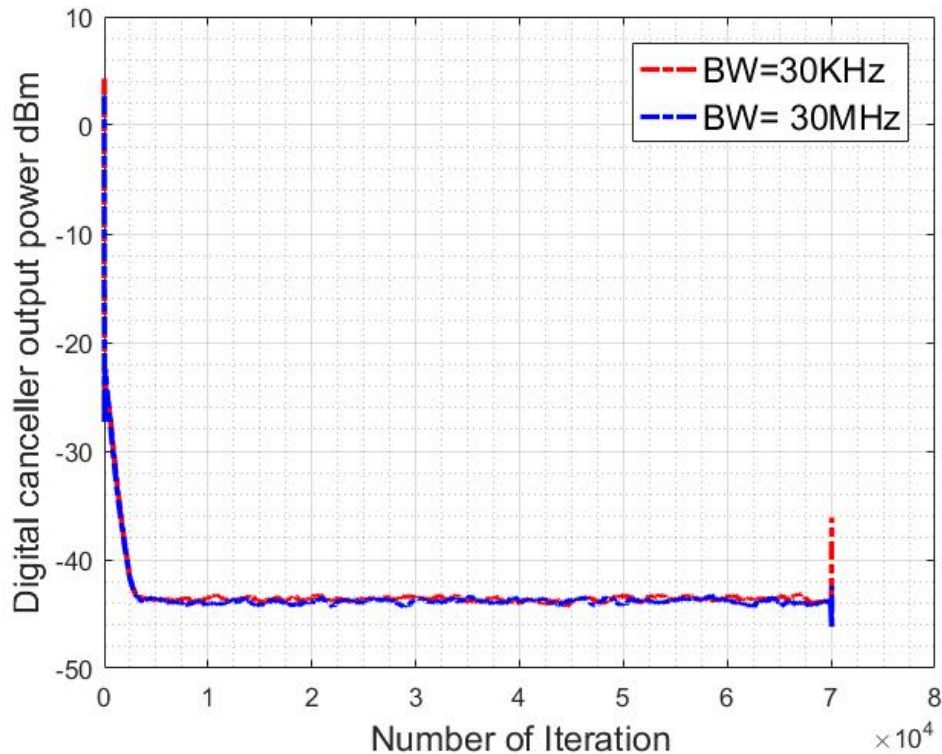

Figure 6.6: The instantaneous and average power of digital canceller output for narrow and wideband signal.

The number of training samples and step size has been fixed to 7×10^4 samples and the 0.7 respectively. The up sampling factor has been chosen 4 for both narrow band and wideband signal. It can be seen from *Figure 6.6*, the amount of SI cancellation is same for a narrow band signal and wideband signal. The minimum digital canceller output power has been observed to be about -44.31dBm.

6.5 Effect of Length of Estimation Filter

In the next experiment set up, effect of length of adaptive filter has been studied by varying the length of adaptive filter with constant number of training samples and step size. The impulse response of SI channel consists of 3 taps. It can be seen from *Figure 6.7*, when there is a single tap in estimation filter there is less SI attenuation whereas increasing the length of the estimation filter has improved the SI attenuation. This means that

the filter length should be equal to the number of significant taps in the impulse response of SI channel.

A small filter length has increased the convergence speed whereas a longer filter length has decreased the convergence speed. However, at some point increasing the filter length does not increase the SI attenuation. The power of error signal at M=1 and M=3 was observed to be -11.12 dBm and -43.41dBm. The power of error signal at M=9 was observed to be -39.41dBm.
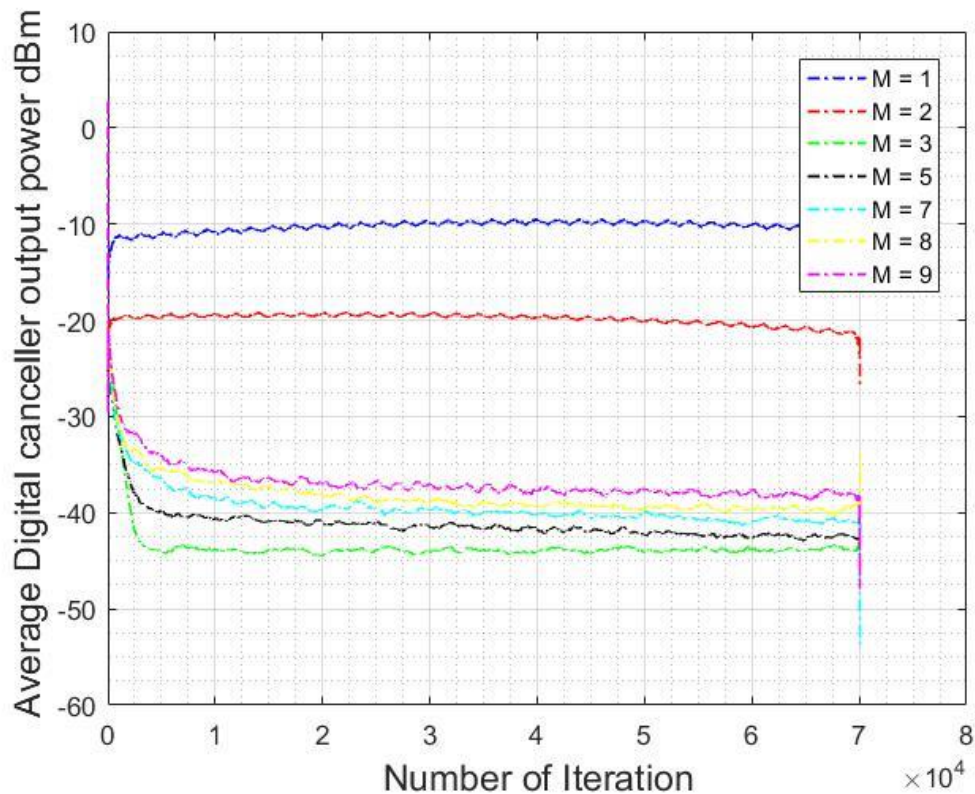

Figure 6.7: The average power of digital canceller output for different length of adaptive filter.

6.6 Effect of K parameter of SI Channel

In the next experiment set up, effect of Rician K parameter on SI attenuation has been studied with the channel parameters specified in table 3.1 and table 3.2. The number of samples were kept constant to 7×10^4 samples and the step size μ was kept constant with a value of 0.7. It can be seen from the *Figure 6.8*, the amount of digital canceller power has started to decrease with increase in the amount of K parameter.

As mentioned before, K parameter signifies the ratio of power of LOS component to the power of other reflected component. Lower K means that the power from LOS component has been decreased with respect to other reflected component, which results in decrease in weight gain of LOS component of SI channel, whereas there is significant

increase in the weight gain of other reflected component. The output power of digital canceller was observed minimum at K=10dB with a value of about -47.5dBm. The value of digital canceller for K= 40, 50 and 60 dB was observed to be about -45dBm.
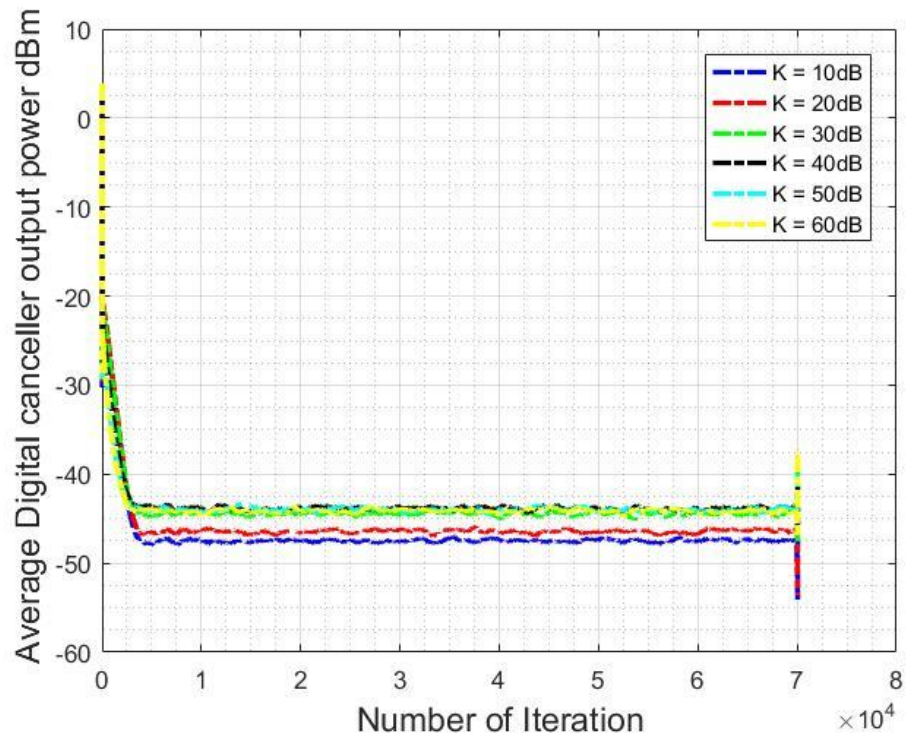

Figure 6.8: The average power of digital canceller output for different value of K.

7 Conclusion and Future Work

In this thesis, the effect of LMS algorithm and SI channel on digital SI cancellation was studied by varying the parameters for the LMS algorithm and SI channel. A simple baseband transceiver was used in LabVIEW environment to carry out this analysis. The performance of LMS algorithm was based on steady state error and convergence rate.

The waveform result showed that high amount of training samples can give better channel estimation which results in the higher amount of SI attenuation to some level. The SI attenuation cannot be increase beyond certain amount of training samples. The performance of SI canceller was observed similar for a narrowband signal and wideband signal when all SI channel and LMS parameters were held constant.

Increasing the step size to certain threshold has increased the amount of SI attenuation. It is important to choose the right value of step size because increasing the step size to beyond some threshold can result in divergence of error signal, resulting in the lower amount of SI attenuation.

The length of adaptive filter must be equal to the number of taps used in SI coupling channel in order to get the better estimation of channel. So it is important to know the characteristic of SI channel. A longer filter length increases the computational resources than a shorter filter length. However, increasing filter length can only attenuate the SI signal to some threshold. A small filter length can increase the convergence speed.

The K parameter of Rician channel controls the amount of SI cancellation that can be achieved using adaptive algorithm. A better estimation of SI channel was observed when the K parameter value was equal to 10dB for a fixed amount of step size and training samples.

In this thesis, LMS algorithm was design for a complex signal which was processed as a real valued signal. The same design can be used to program a LabVIEW FPGA with a fixed point implementation. The SI cancellation can be done in real time using National Instrument Flex RIO system. LMS algorithm suffers from Eigen value spread which results in the instability of the adaptive filter. Compared to LMS, Recursive Least Square (RLS) algorithms have a faster convergence speed and do not exhibit the eigenvalue spread problem. However, computational complexity of RLS algorithm increases because of the complicated mathematical operations. This thesis work can also be implemented using RLS algorithm.

REFERENCES

[1] V.A. Dubendorf, *A History of Wireless Technologies*. John Wiley & Sons, Ltd, 2003.

[2] J.I. Choi, M. Jain, K. Srinivasan, P. Levis and S. Katti, "Achieving Single Channel, Full Duplex Wireless Communication," in *Proc.MOBICOM.* Citeseer, 2010, pp:1-12.

[3] P.M. Awachat and S.S Godbole, "A Design Approach for Noise Cancellation in Adaptive LMS Predictor Using MATLAB," in *International Journal of Engineering Research and Applications* (IJERA),2(4), pp: 2388-2391, 2012.

[4] J.R. Krier and I.F. Akyildiz, "Active Self-Interference Cancellation of Passband Signal Using Gradient Descent," in *IEEE 24th International symposium on personal, indoor and mobile radio communication: Fundamentals and PHY track*, pages: 1212-1216, 2013.

[5] LabVIEW System Design Software. URL: http://www.ni.com/labview/. Visited at 2015-11-06.

[6] M. Duarte and A. Sabharwal, "Full Duplex Wireless Communication Using off the Shelf Radios: Feasibility and First Results," in *44th Asilomar Conference on Signals, Systems & Computers,* 2010, pp: 1558-1562.

[7] M. Jain, J.I. Choi, T.M. Kim, D. Bhardia, S. Seth, K. Srinivasan, P. Levis, S. Katti, and P. Sinha, "Practical, Real-Time, Full Duplex Wireless," in *17th Annual International Conference on Mobile computing and Networking*, Mobicom'11, pages: 1-12, Las Vegas, Nevada, USA, 2011.

[8] W. Cheng, X. Zhang and H. Zhang, "Full Duplex Spectrum Sensing in Non-Time-Slotted Cognitive Radio Networks," *Military Communications Conference-Track2-Network Protocols and Performance*, pages 1029-1034, 2011.

[9] C.E. Shannon, *A Mathematical Theory of Communication*. The Bell System Technical Journal, 27, 1948.

[10] S. Haykin, *Adaptive Filter Theory*. Prentice-Hall, Inc., 2007.

[11] R. Jain, Channel Models: A Tutorial, pages 1-21, 2007.

[12] Universal Mobile Telecommunications System(UMTS); UTRAN Architecture for 3G Home Node B(HNB); stage 2(3GPP TS 25.467 version 11.4.0 release 11). ETSI, Sophia Antipolis Cedex, France.

[13] A. Sahai, G. Patel and A. Sabharwal, "Pushing the limits of Full-duplex: Design and Real-time Implementation," Department of Electrical and Computer Engineering, Rice University, Technical Report TREE1104, 2011.

[14] J. Zhang, L. Fu and X. Wang, "Asymptotic Analysis on Secrecy Capacity in Large-Scale Wireless Networks," *IEEE/ACM Transactions on Networking*, 22(1):66-79, 2014.

[15] G. Zheng, I. Krikidis, J. Li, A.P. Petropulu and B. Ottersten, "Improving physical layer secrecy using full-duplex jamming receivers," *IEEE Transactions on Signal Processing*, 61(20):4962-4973, 2013.

[16] E. Everett, M. Duarte, C. Dick and A. Sabharwal. Empowering, "Empowering Full-Duplex Wireless Communication by Exploiting Directional Diversity," in *45th Asilomar Conference on Signals, Systems & Computers*, 2011.

[17] L. Antilla, D. Korpi, V. Syrjala, M. Valkama, "Cancellation of Power Amplifier Induced Nonlinear Self-Interference in Full-Duplex Transceivers," Department of Electronics and Communication Engineering, Tampere University of Technology, Finland, pages 1-6.

[18] M. Duarte, C. Dick and A. Sabharwal, "Experiment-Driven Characterization of Full-Duplex Wireless Systems," *In IEEE Transactions on Wireless Communications*,11(12): 4296-4307, 2012.

[19] E. Ahmed, A.M. Eltawil and A. Sabharwal, "Self Interference Cancellation with Nonlinear Distortion Suppression for Full- Duplex System," in *Proc. Asilomar Conference on Signals, Systems & Computers,* 2013.

[20] C.A. Balanis, *Antenna Theory*. John Wiley & Sons, Inc., 2005.

[21] T. Rappaport, *Wireless Communications: Principle and Practice.* Prentice-Hall, Inc., 2001.

[22] G.D. Durgin and T.S. Rappaport, "Theory of Multipath Factors for Small-Scale Fading Wireless Channels," in *IEEE Transactions on Antennas and Propagation*, 48(5):682-693, 2000.

[23] R. Steele and L. Hanzo, *Mobile radio Communications*. Pentech press London,1992, vol 3.

[24] LabVIEW Help Tool. LabVIEW 2015, National Instrument.

[25] P. Dent, G.E. Bottomley and T. Croft, "Jake's Fading Model Revisited," *Electronics letters*, vol 29, No.13, 24th June 2013.